杜立配

McGILL U / UC BERKELEY / LBNL

MULTI-MESSENGER HEAVY-ION COLLISION PHYSICS AT BEAM ENERGY SCAN ENERGIES

中国科学院大学

JUNE 14, 2024

QCD PHASE DIAGRAM

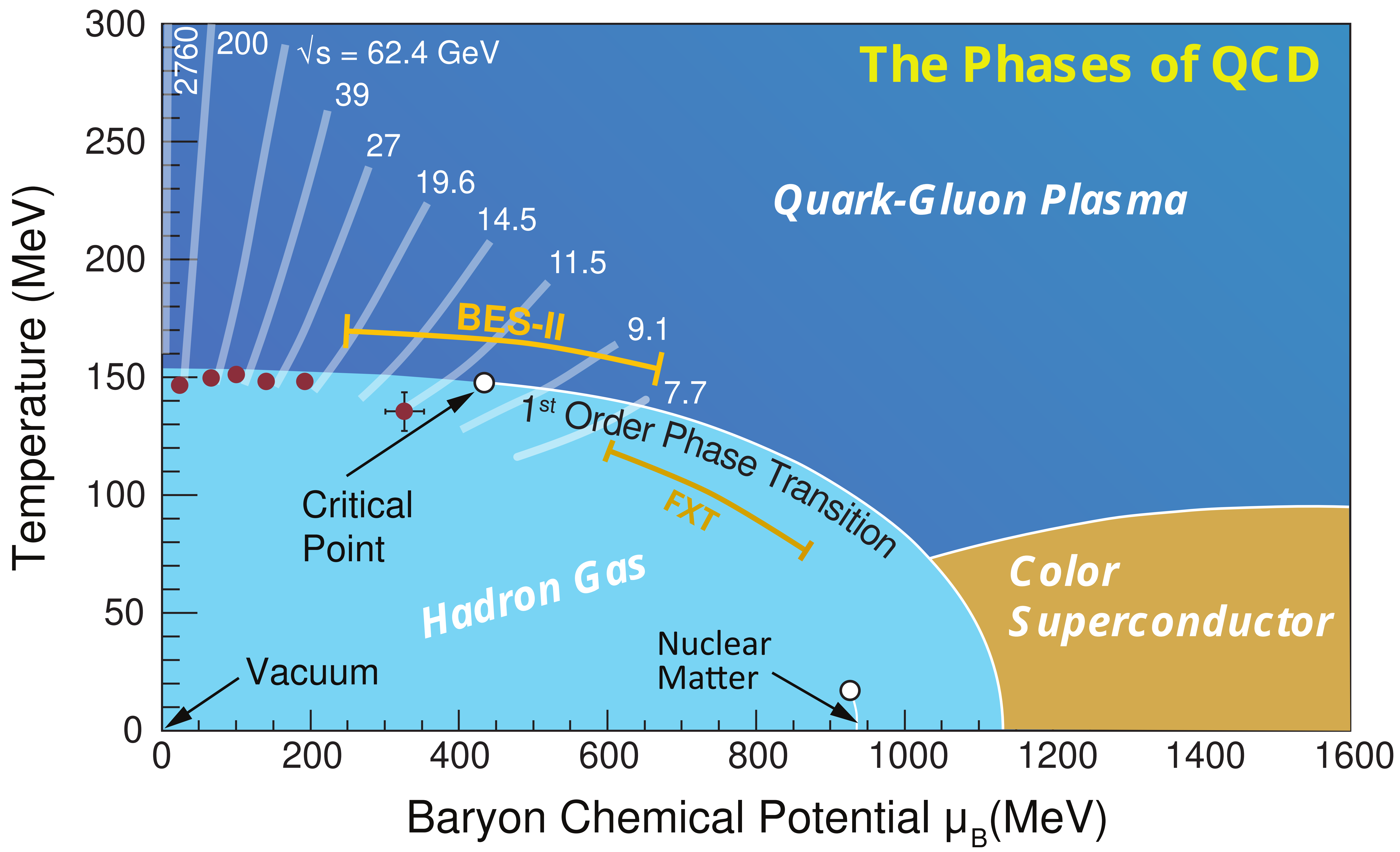

fig: Du, Sorensen, and Stephanov, 2402.10183, modified from Bzdak, Esumi, Koch, Liao, Stephanov, and Xu, Phys. Rept. 853 (2020)

- Heavy-ion collisions at varying beam energies are essential for probing the QCD phase diagram.

MULTI-MESSENGER HEAVY-ION COLLISION PHYSICS

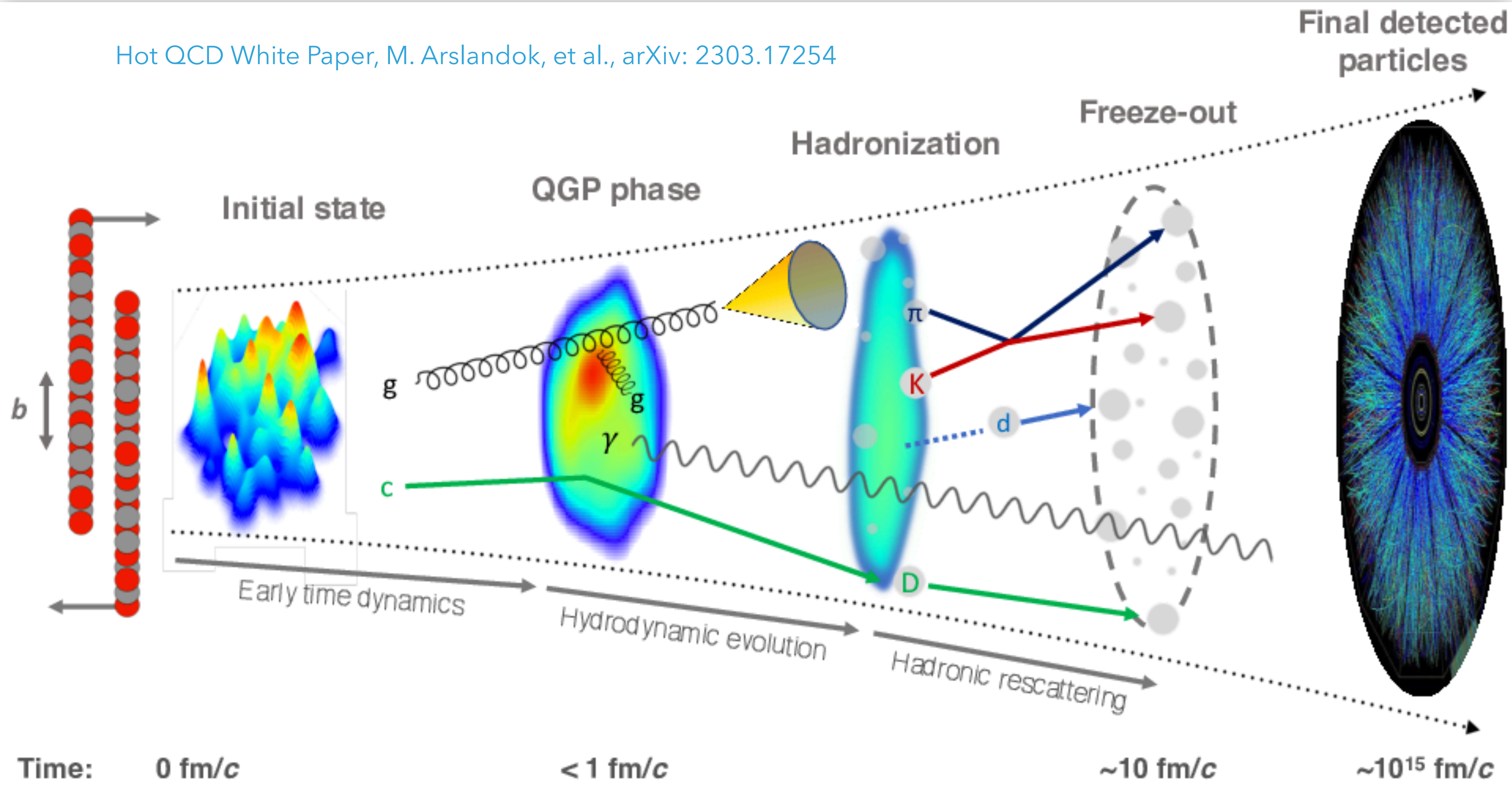

Review Article | Published: 03 October 2019

Multi-messenger astrophysics

Péter Mészáros, Derek B. Fox, Chad Hanna & Kohta Murase

Nature Reviews Physics 1, 585–599 (2019) | Cite this article

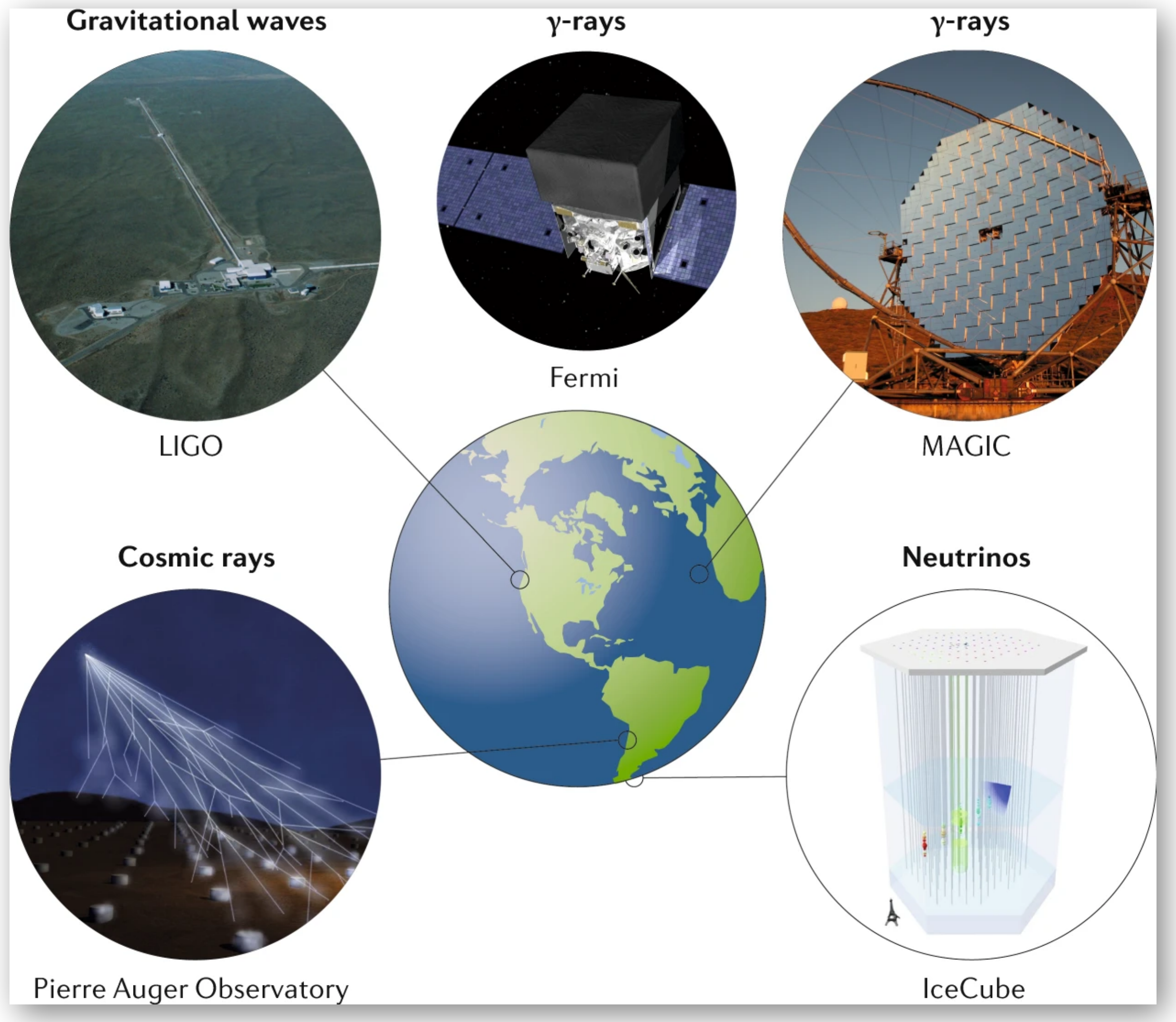

- Three main categories of observables in heavy-ion collisions:
  - soft hadrons
  - hard probes: jets & heavy quarks
  - electromagnetic probes

SOFT HADRON OBSERVABLES

MID-RAPIDITY MEASUREMENTS

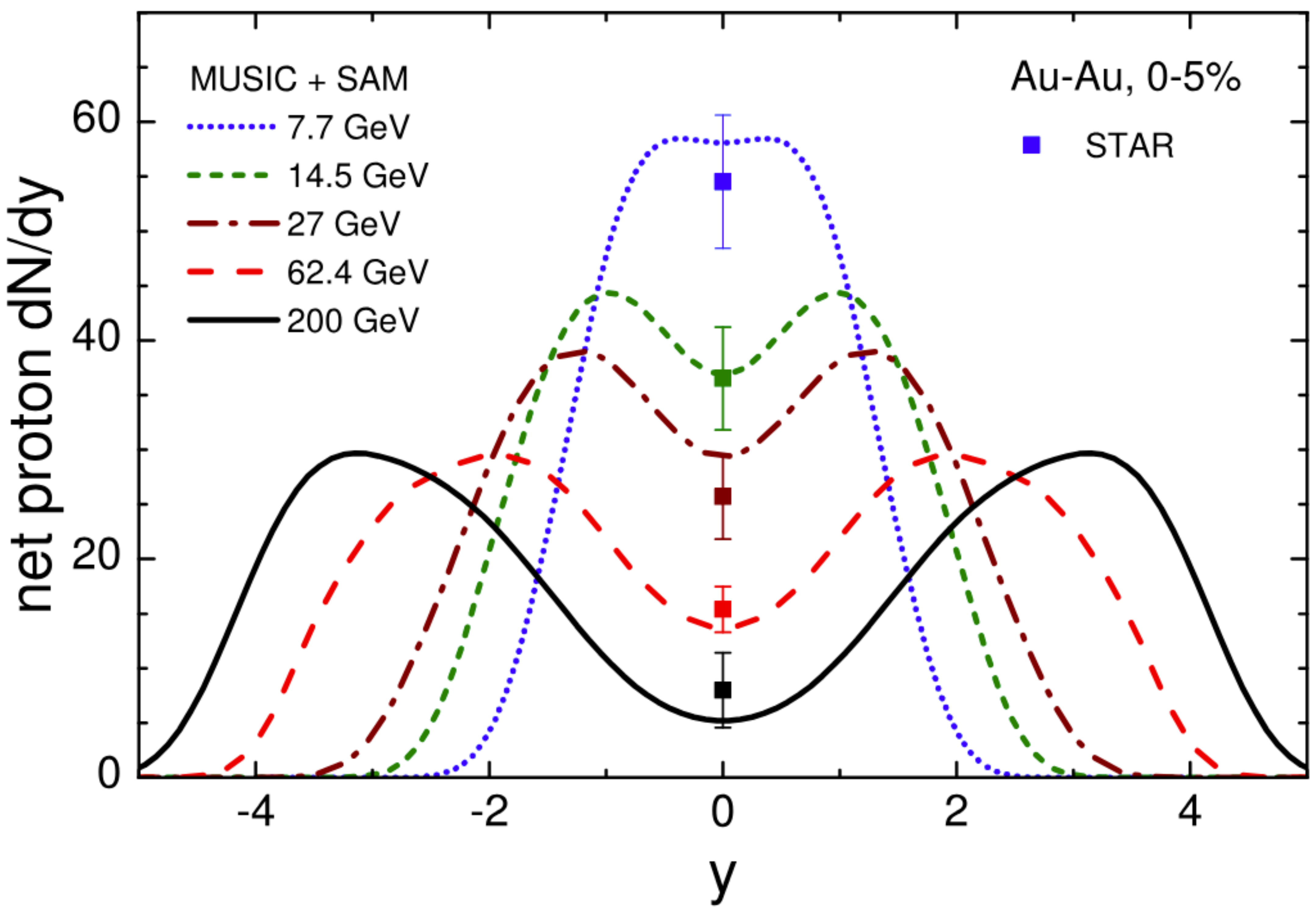

Vovchenko, Koch, and C. Shen, PRC 105, 014904 (2022)

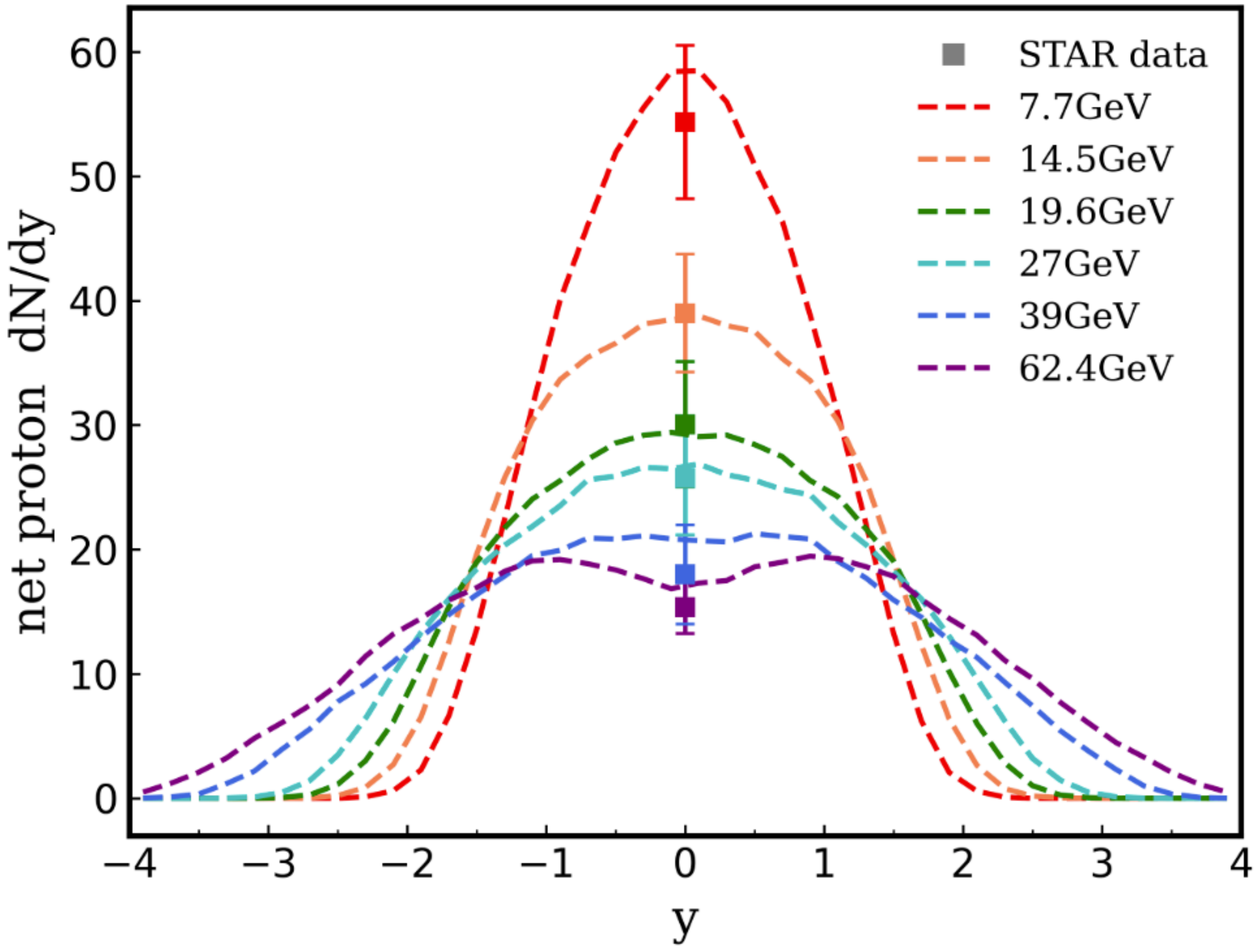

Y.-f. Shen, Chen, Wu, Xu, and Huang, 2404.02397

- If we only take measurements at mid-rapidity, the dynamics along the beam direction may not be well-constrained.

G. Denicol et al, PRC 98, 034916 (2018); **LD**, An and Heinz, PRC 104, 064904 (2021); **LD**, Gao, Jeon & Gale, PRC 109, 014907 (2024); Mendenhall and Lin, PRC 107, 034909 (2023); Cimerman, Karpenko, Tomášik, and Trzeciak, PRC 103, 034902 (2021); Cimerman, Karpenko, Tomášik, and Huovinen, PRC 107, 044902 (2023)

CONSTRUCT RAPIDITY-DISTRIBUTION: $dN^{\mathrm{ch}}/d\eta$

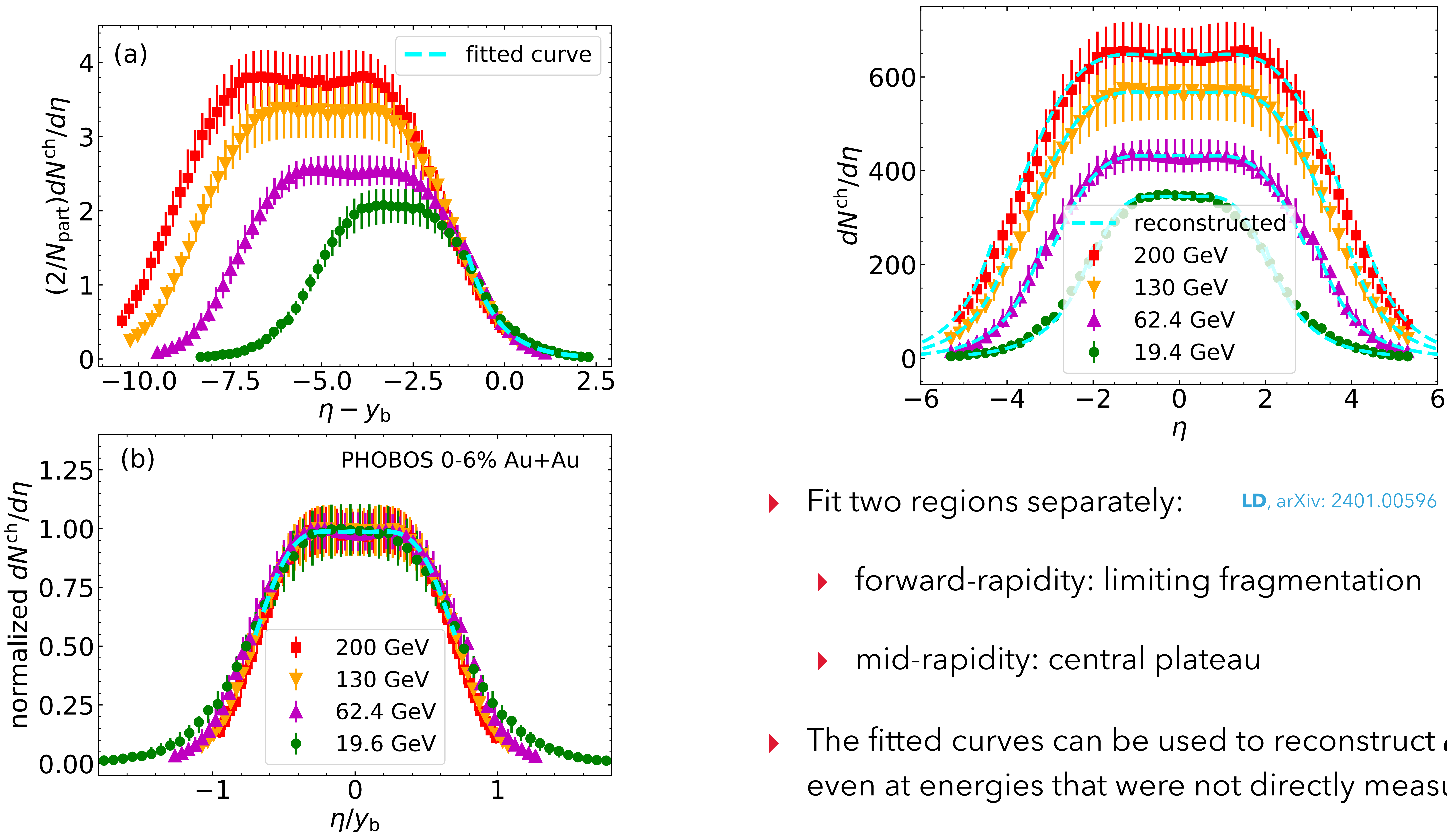

- Fit two regions separately: **LD**, arXiv: 2401.00596
  - forward-rapidity: limiting fragmentation
  - mid-rapidity: central plateau
- The fitted curves can be used to reconstruct $dN^{\mathrm{ch}}/d\eta$, even at energies that were not directly measured.

PHOBOS, PRL 91, 052303 (2003); PHOBOS, PRC 83, 024913 (2011); ALICE, PRL 116, 222302 (2016); Basu et al 2021 J. Phys. G: Nucl. Part. Phys. 48 025103;

CONSTRUCT RAPIDITY-DISTRIBUTION: $dN^{p-\bar{p}}/dy$

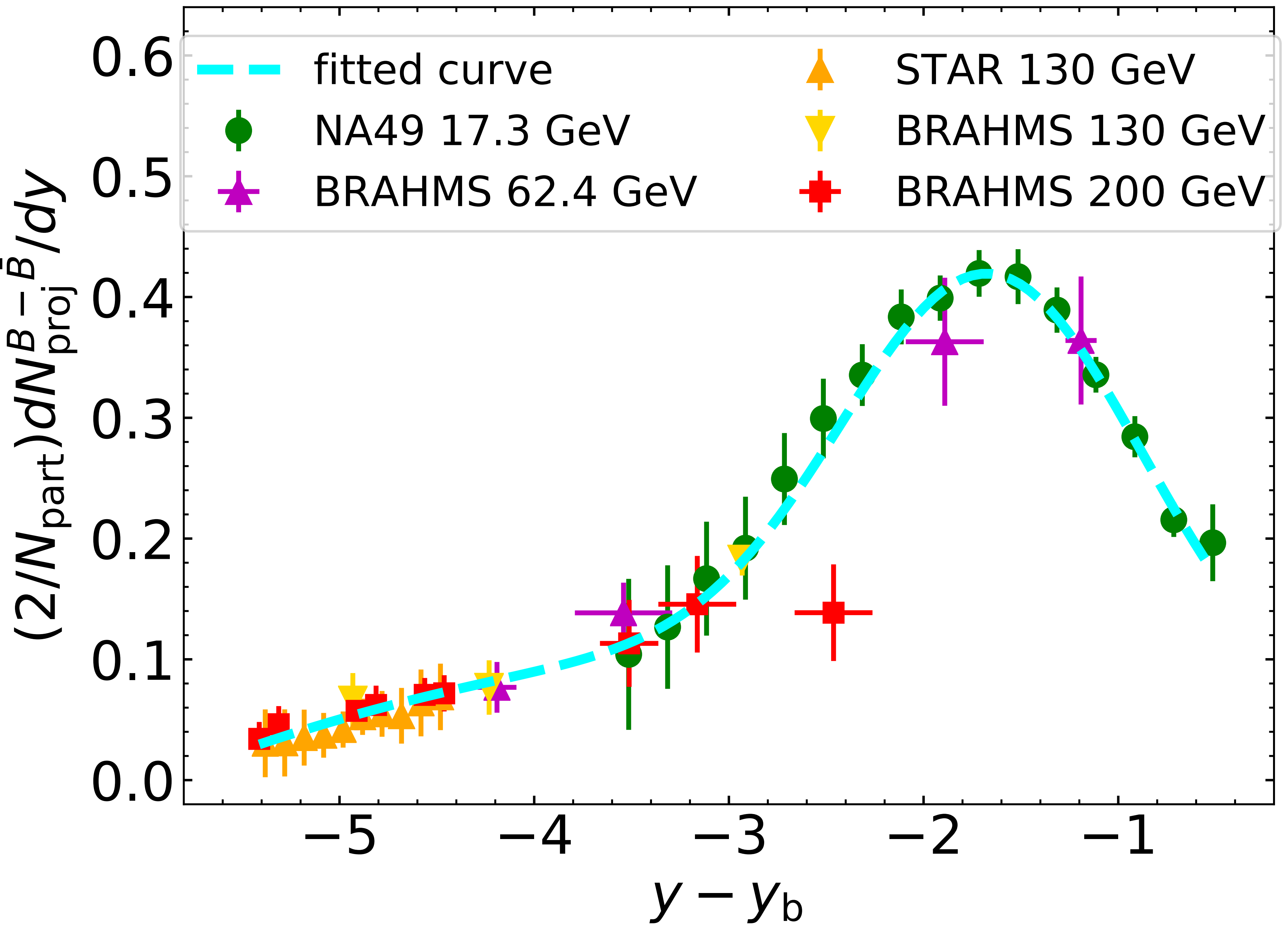

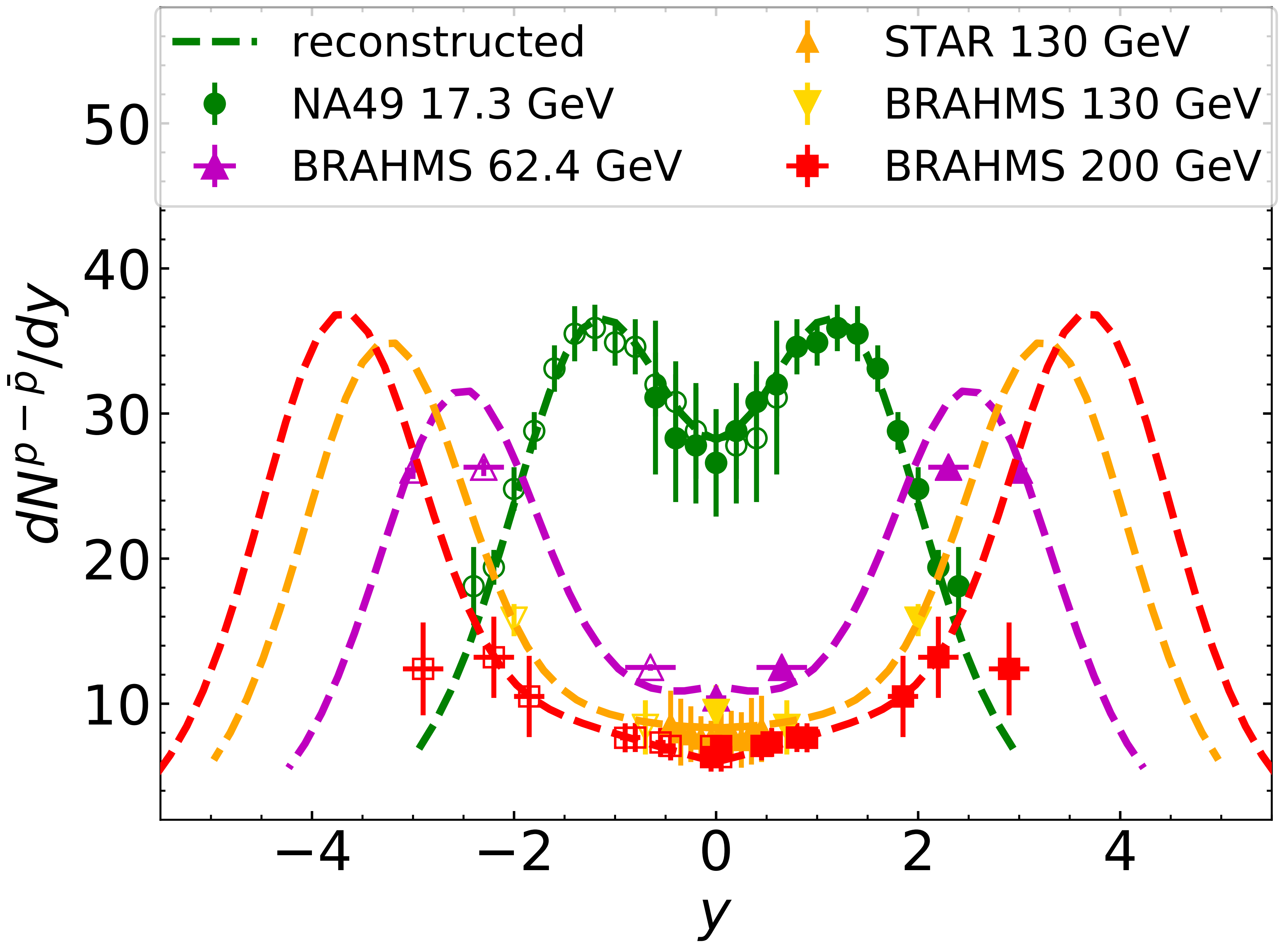

LD, arXiv: 2401.00596

- Fit the net baryon rapidity density attributed to the projectile after subtraction of the target contribution.
- The reconstructed distributions can help constrain models at BES.

BRAHMS, PLB 677, 267-271(2009); Braun-Munzinger, Friman, Redlich, Rustamov, and Stachel, NPA 1008 (2021) 122141; Hoelck, Hiyama, and Wolschin, PLB 840, 137866 (2023)

CONSTRUCT RAPIDITY-DISTRIBUTION: $dN^{p-\bar{p}}/dy$

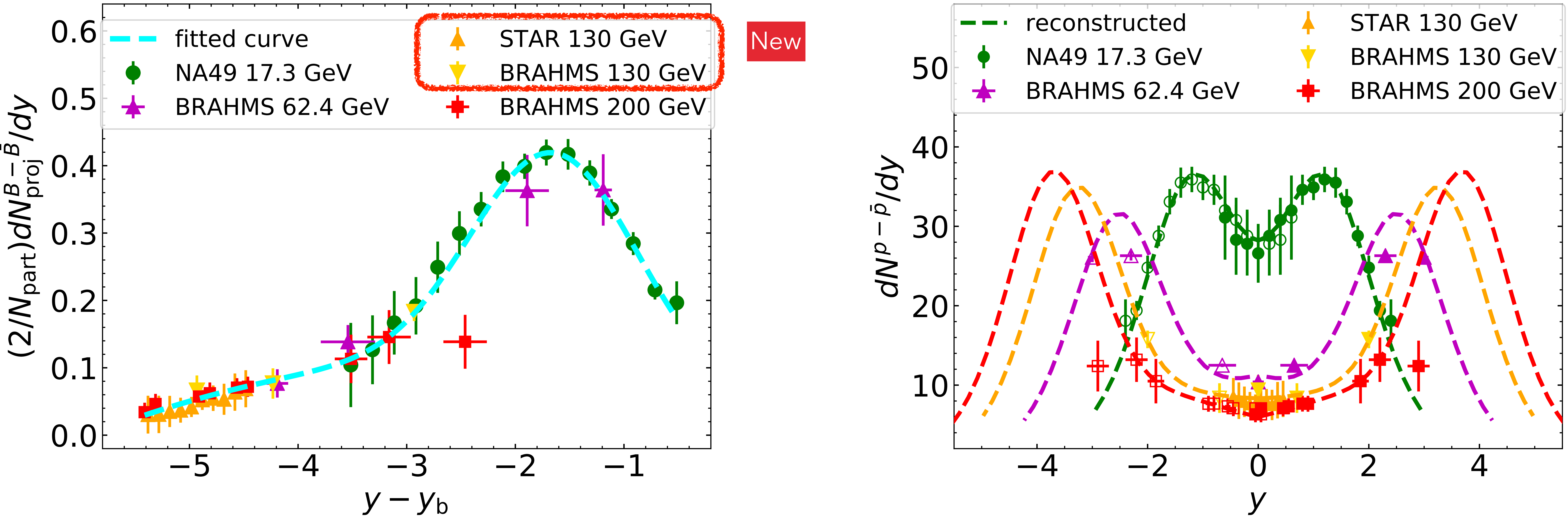

LD, arXiv: 2401.00596

- Fit the net baryon rapidity density attributed to the projectile after subtraction of the target contribution.
- The reconstructed distributions can help constrain models at BES.

BRAHMS, PLB 677, 267-271(2009); Braun-Munzinger, Friman, Redlich, Rustamov, and Stachel, NPA 1008 (2021) 122141; Hoelck, Hiyama, and Wolschin, PLB 840, 137866 (2023)

CONSTRUCT RAPIDITY-DISTRIBUTION: $dN^{p-\bar{p}}/dy$

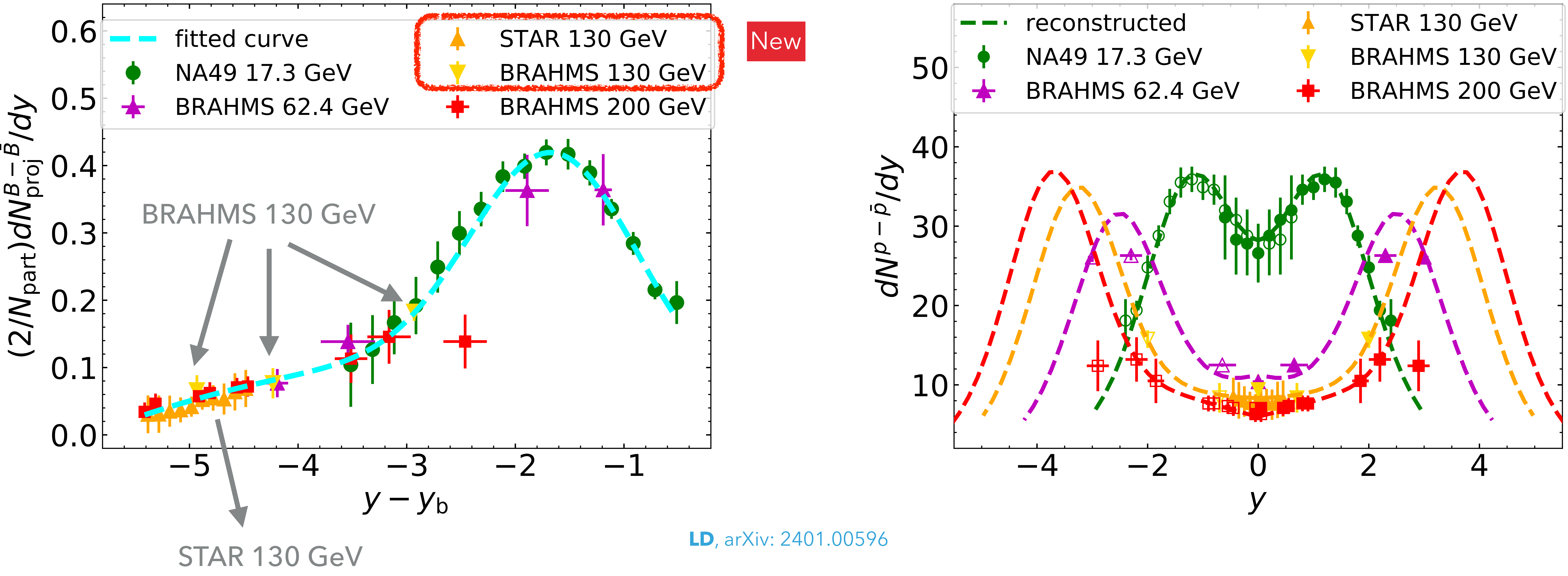

LD, arXiv: 2401.00596

- Fit the net baryon rapidity density attributed to the projectile after subtraction of the target contribution.
- The reconstructed distributions can help constrain models at BES.

BRAHMS, PLB 677, 267-271(2009); Braun-Munzinger, Friman, Redlich, Rustamov, and Stachel, NPA 1008 (2021) 122141; Hoelck, Hiyama, and Wolschin, PLB 840, 137866 (2023)

LONGITUDINAL DYNAMICS

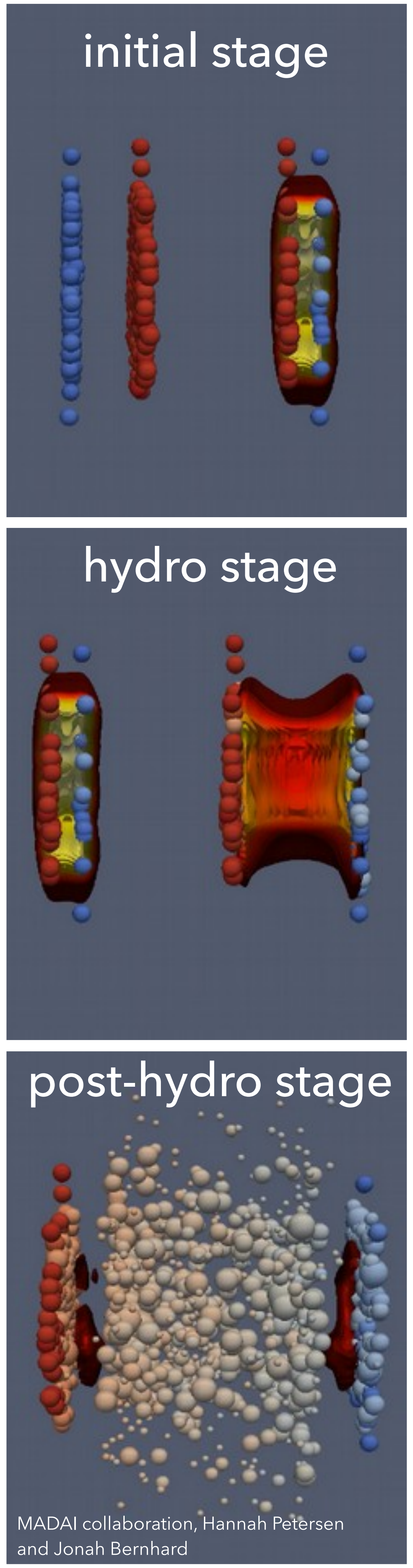

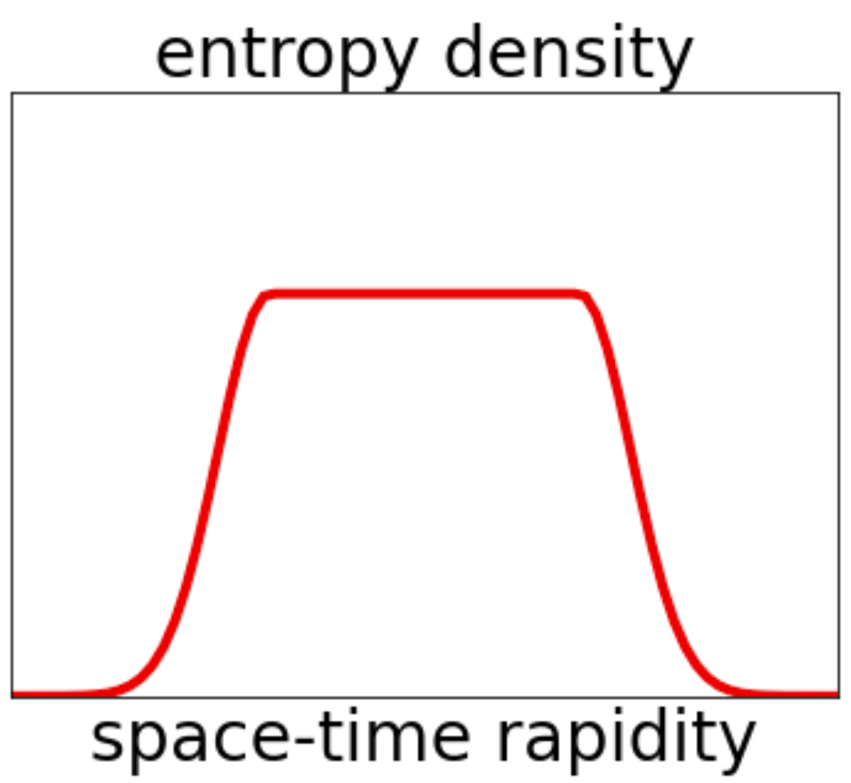

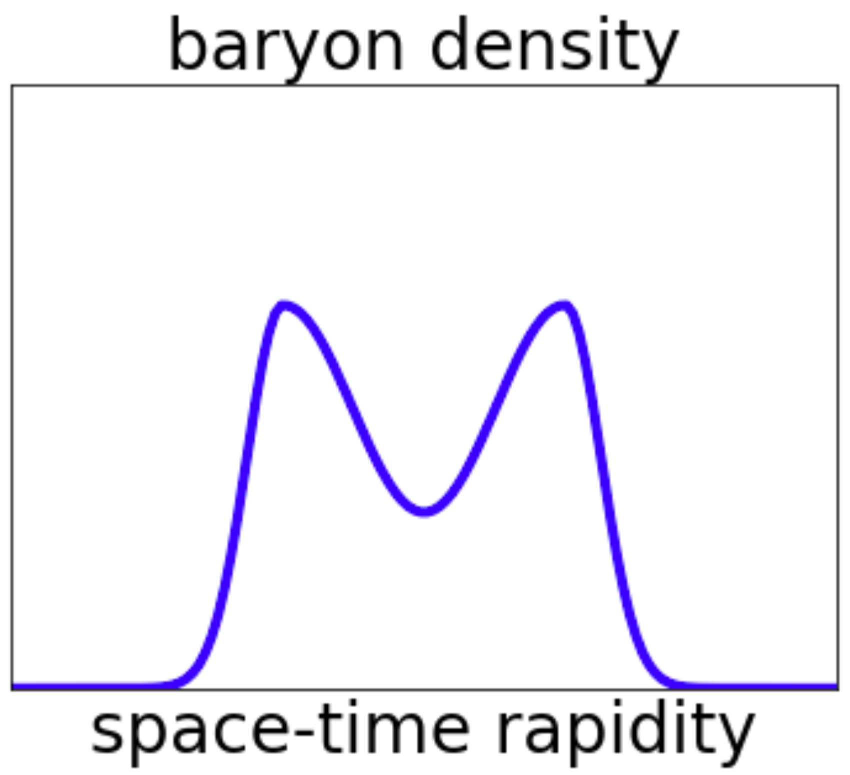

- initial energy deposition
- initial baryon stopping

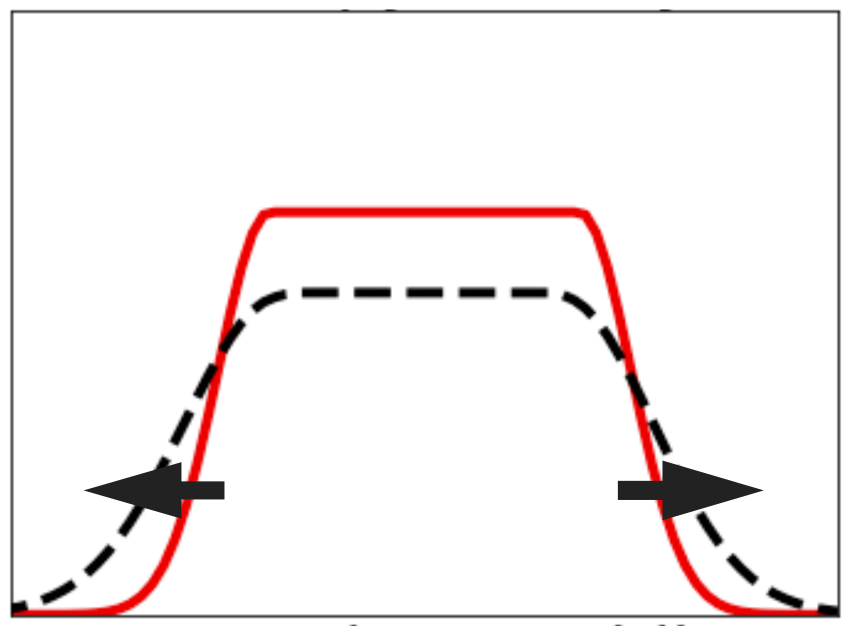

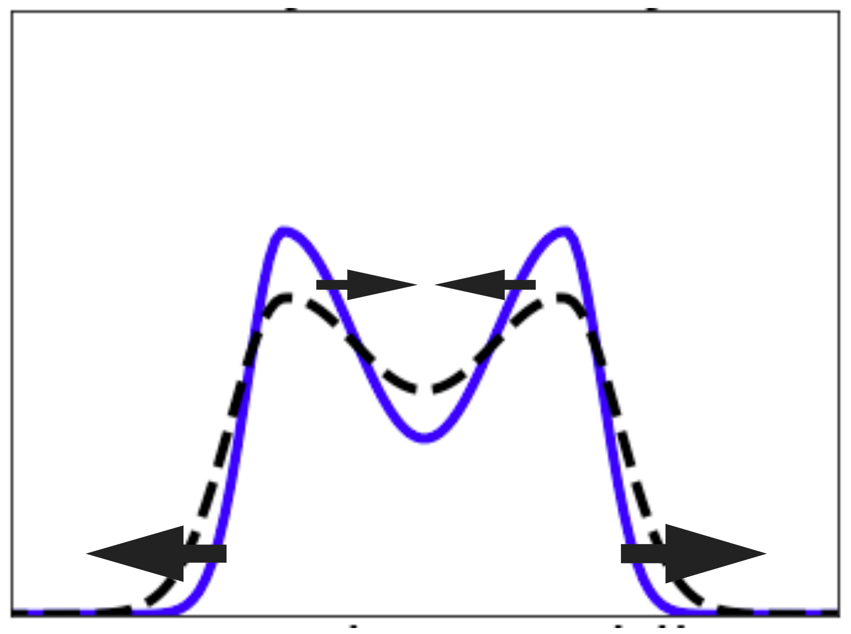

- longitudinal pressure gradient ⟹ longitudinal flow & expansion
- baryon density gradient ⟹ baryon diffusion (hydro transport)

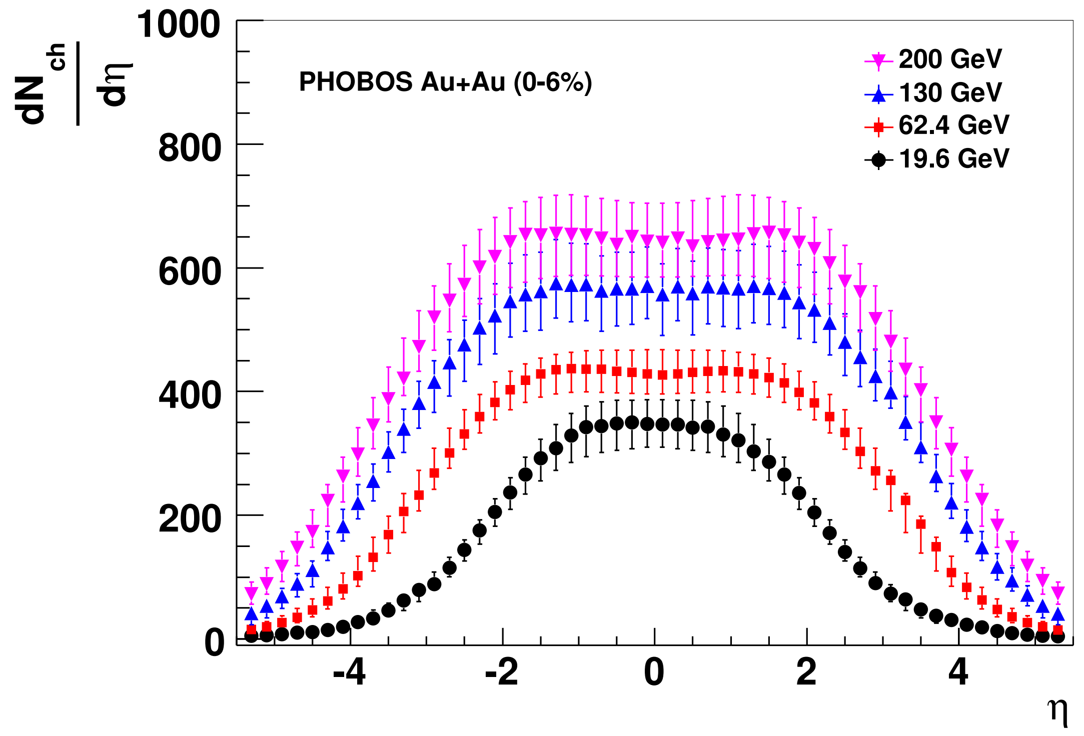

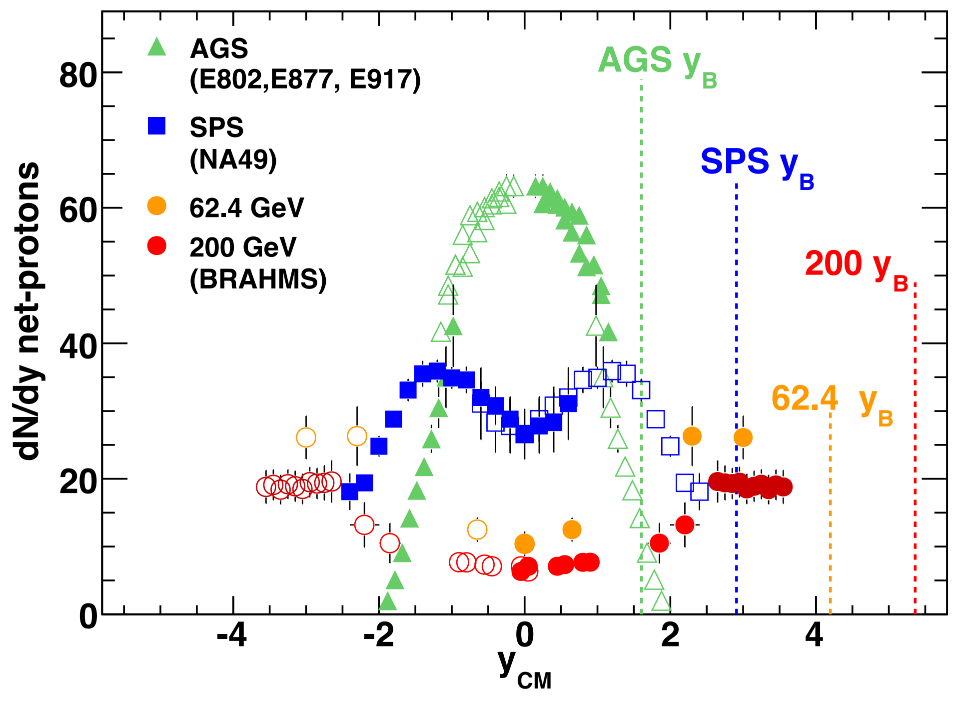

- rapidity-dependent particle distributions

DIRECTED FLOW $v_1(y)$ OF PROTONS

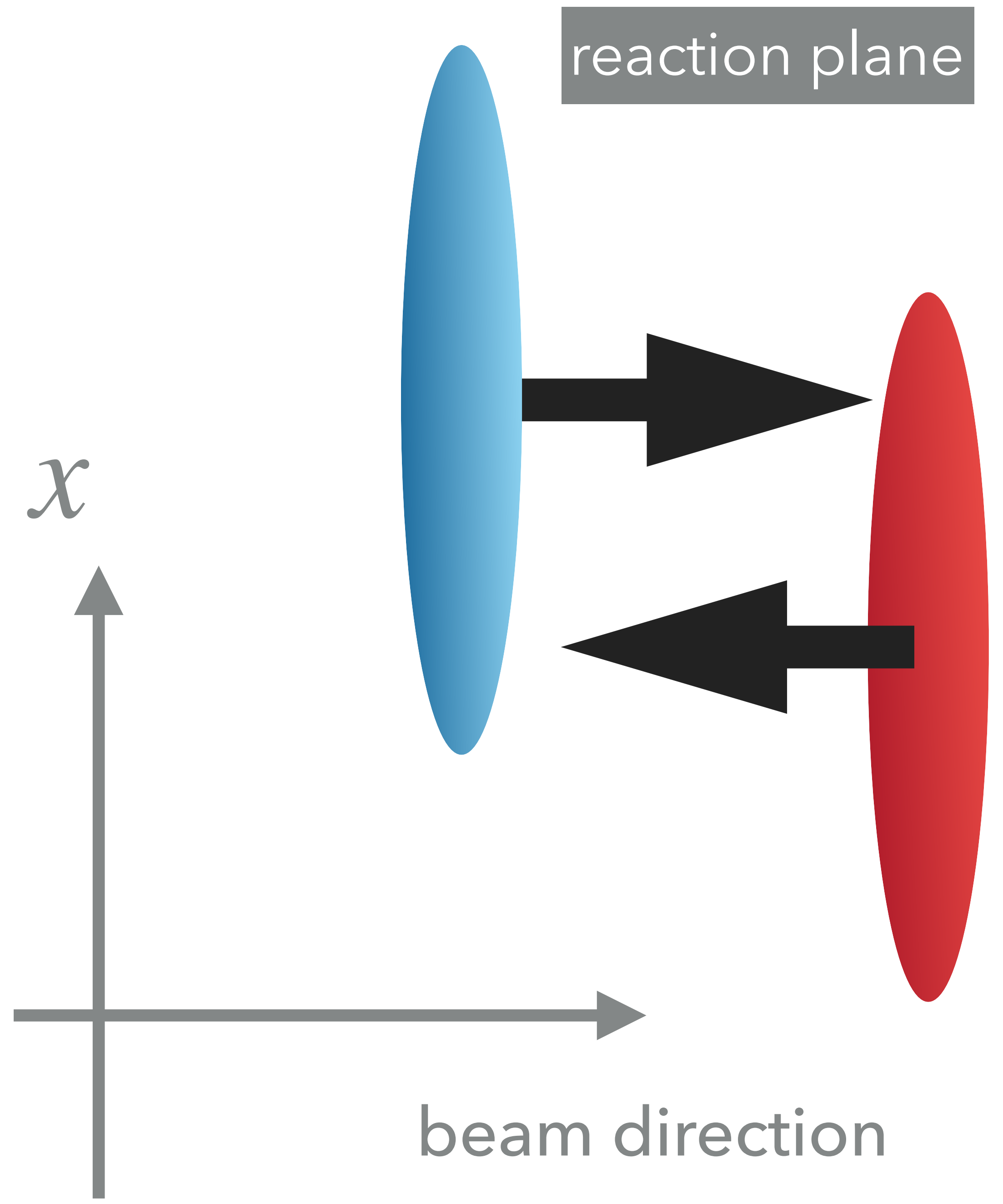

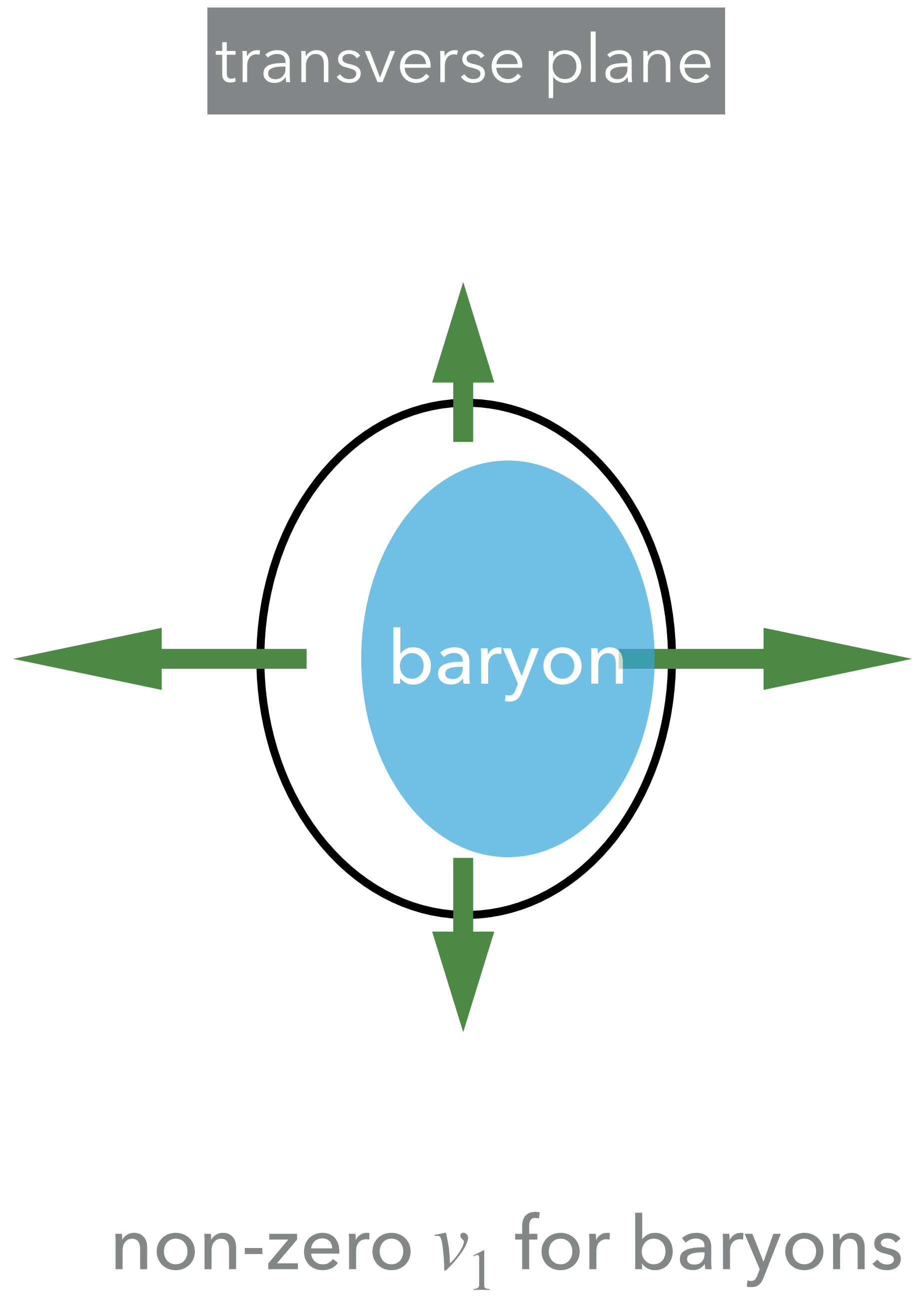

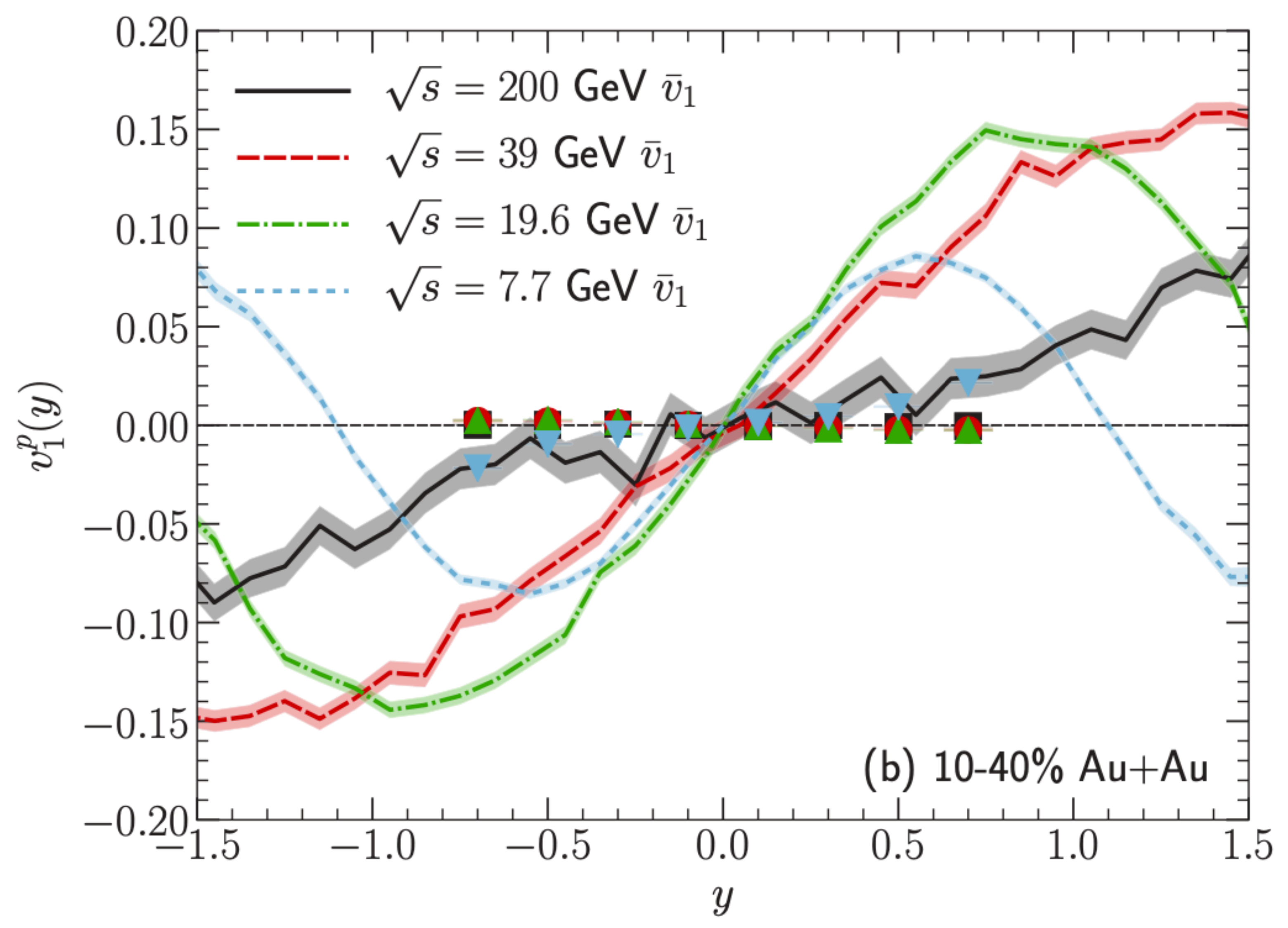

Shen and Alzhrani, PRC102, 014909 (2020)

- $v_1(y)$ of baryons is strongly driven by the asymmetric distribution of baryon density with respect to beam axis + transverse expansion;
- The widely used baryon-stopping picture results in $v_1(y)$ significantly overshooting the experimental measurements for protons at all beam energies.

DIRECTED FLOW $v_1(y)$ OF PROTONS

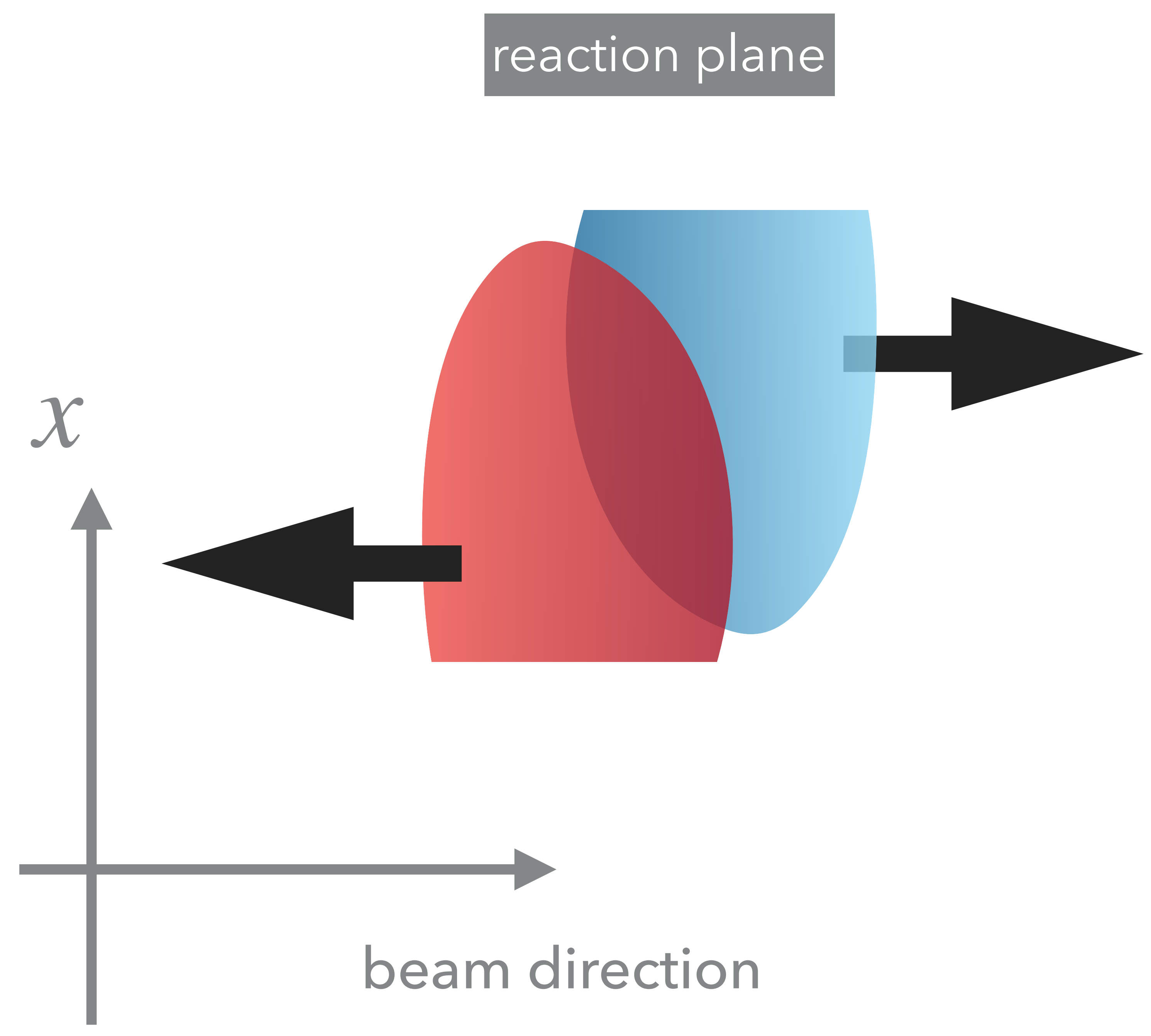

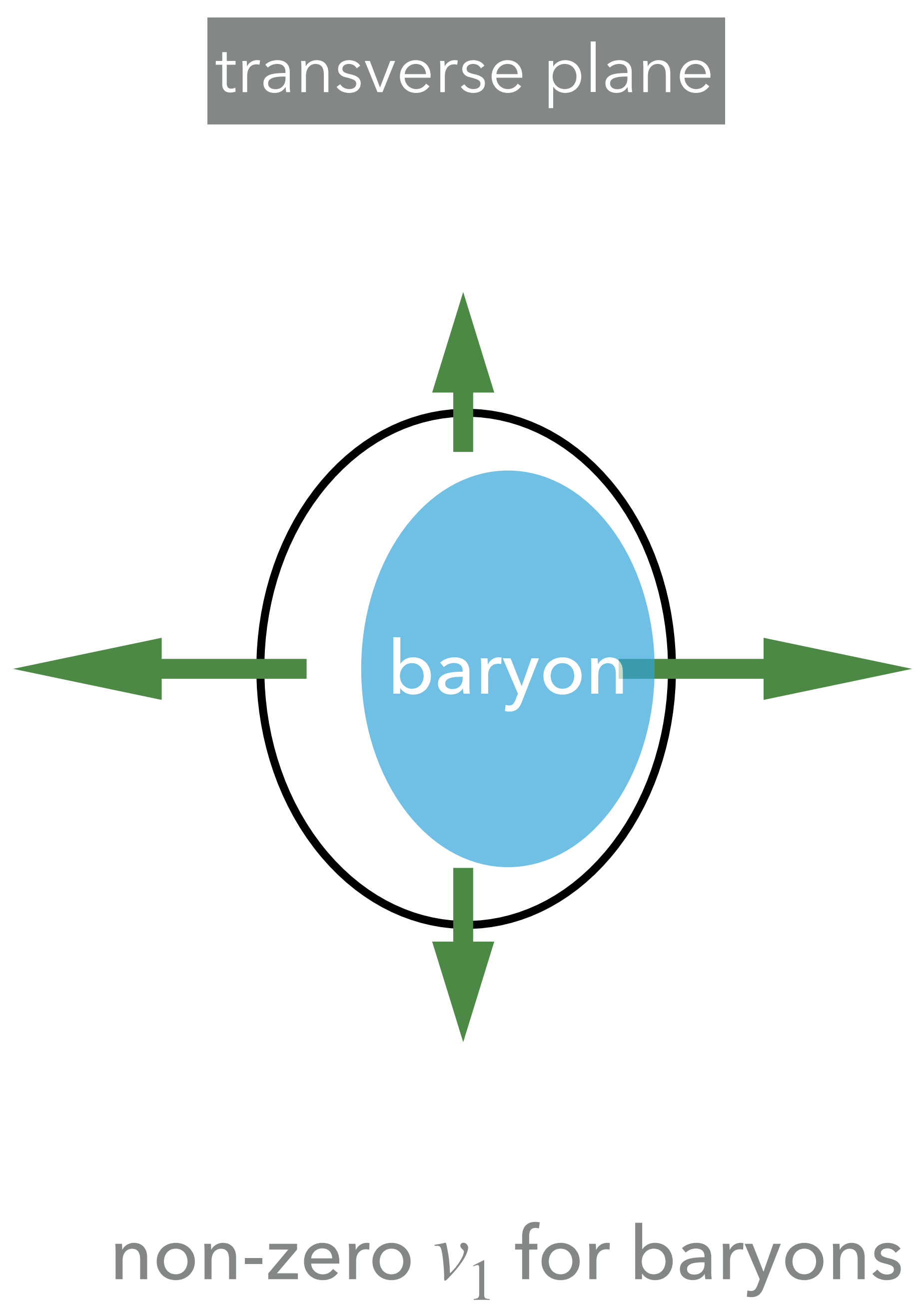

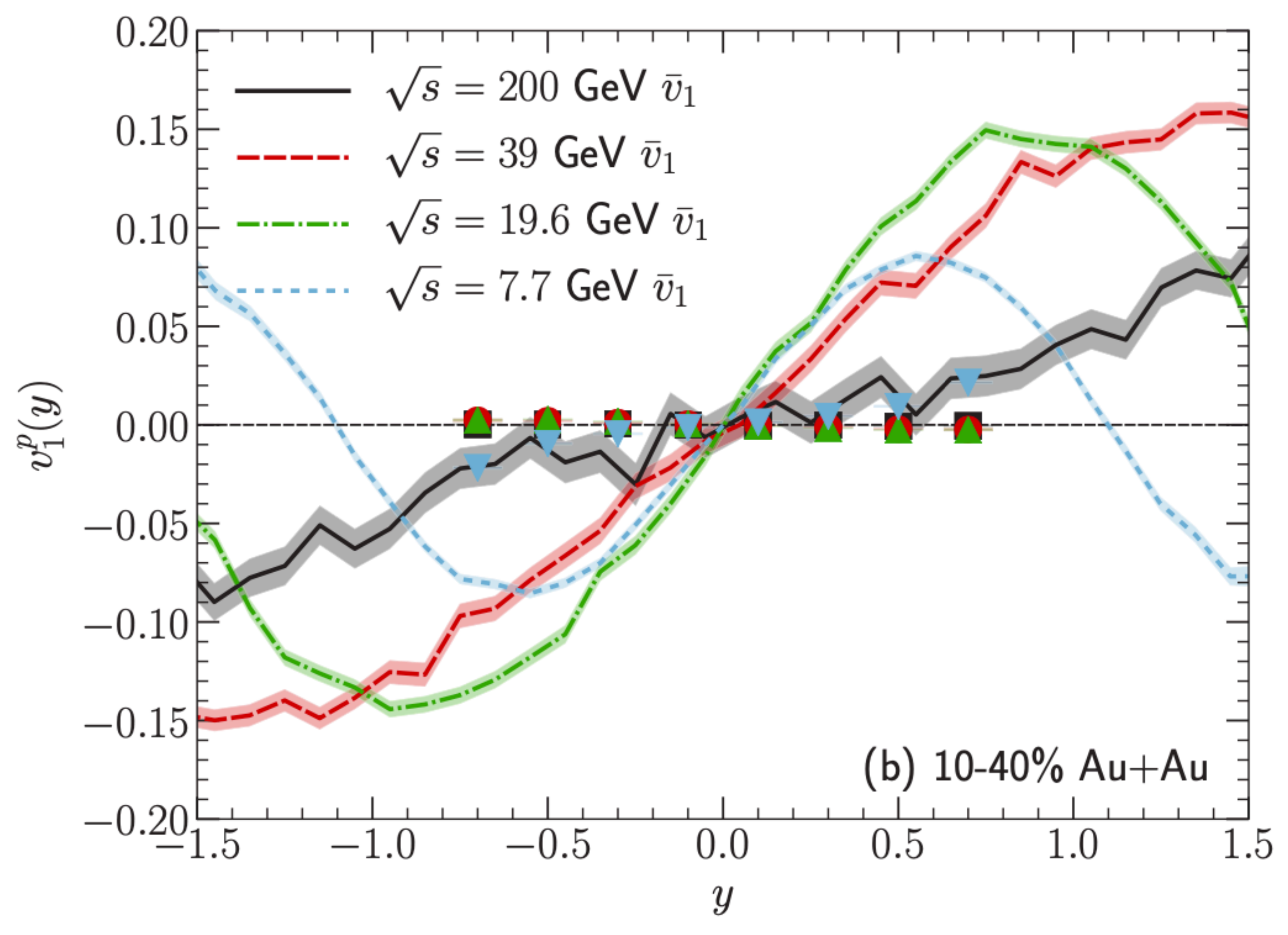

Shen and Alzhrani, PRC102, 014909 (2020)

- $v_1(y)$ of baryons is strongly driven by the asymmetric distribution of baryon density with respect to beam axis + transverse expansion;
- The widely used baryon-stopping picture results in $v_1(y)$ significantly overshooting the experimental measurements for protons at all beam energies.

NEW PARAMETRIC BARYON INITIAL CONDITION

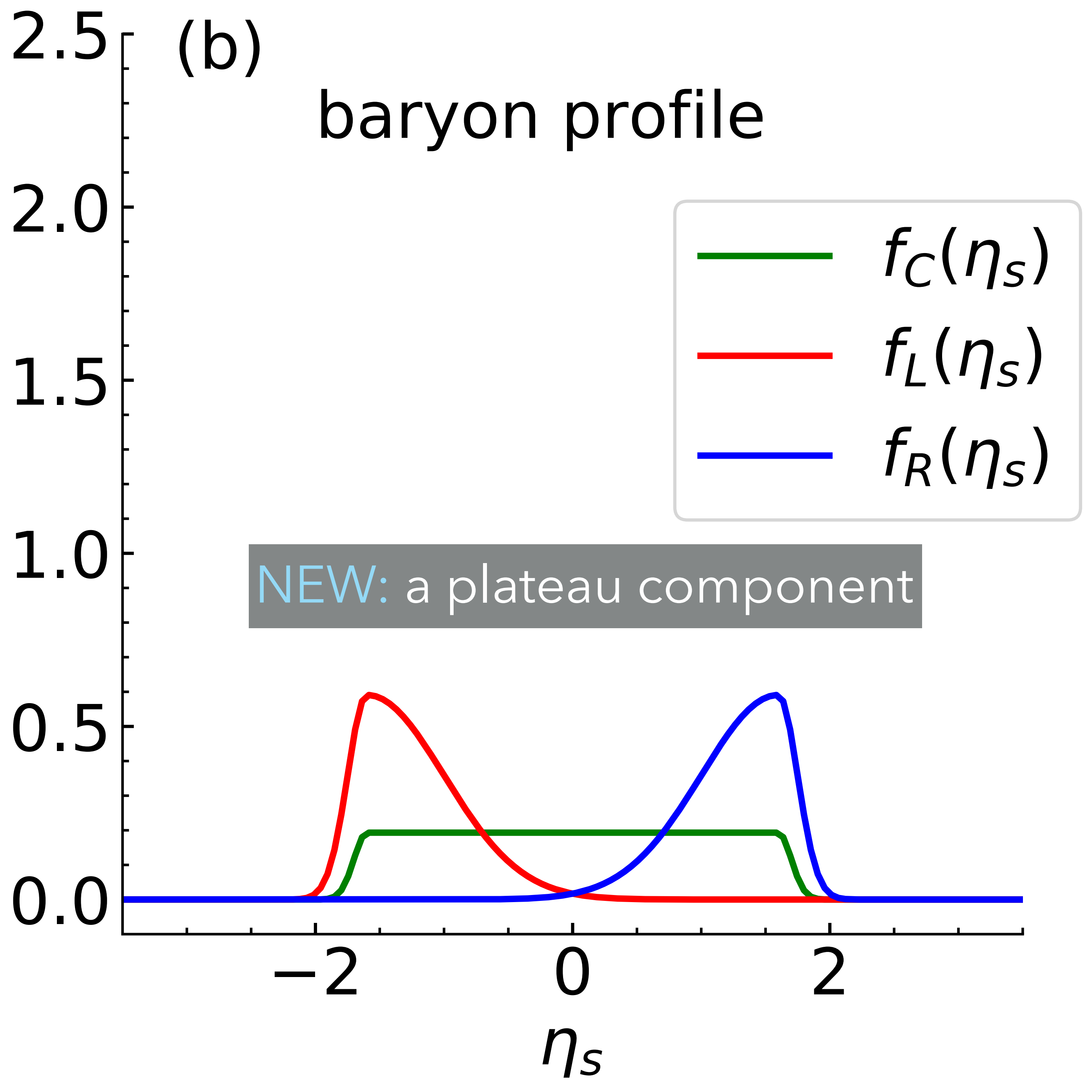

LD, C. Shen, S. Jeon & C. Gale, PRC 108 (2023) L041901

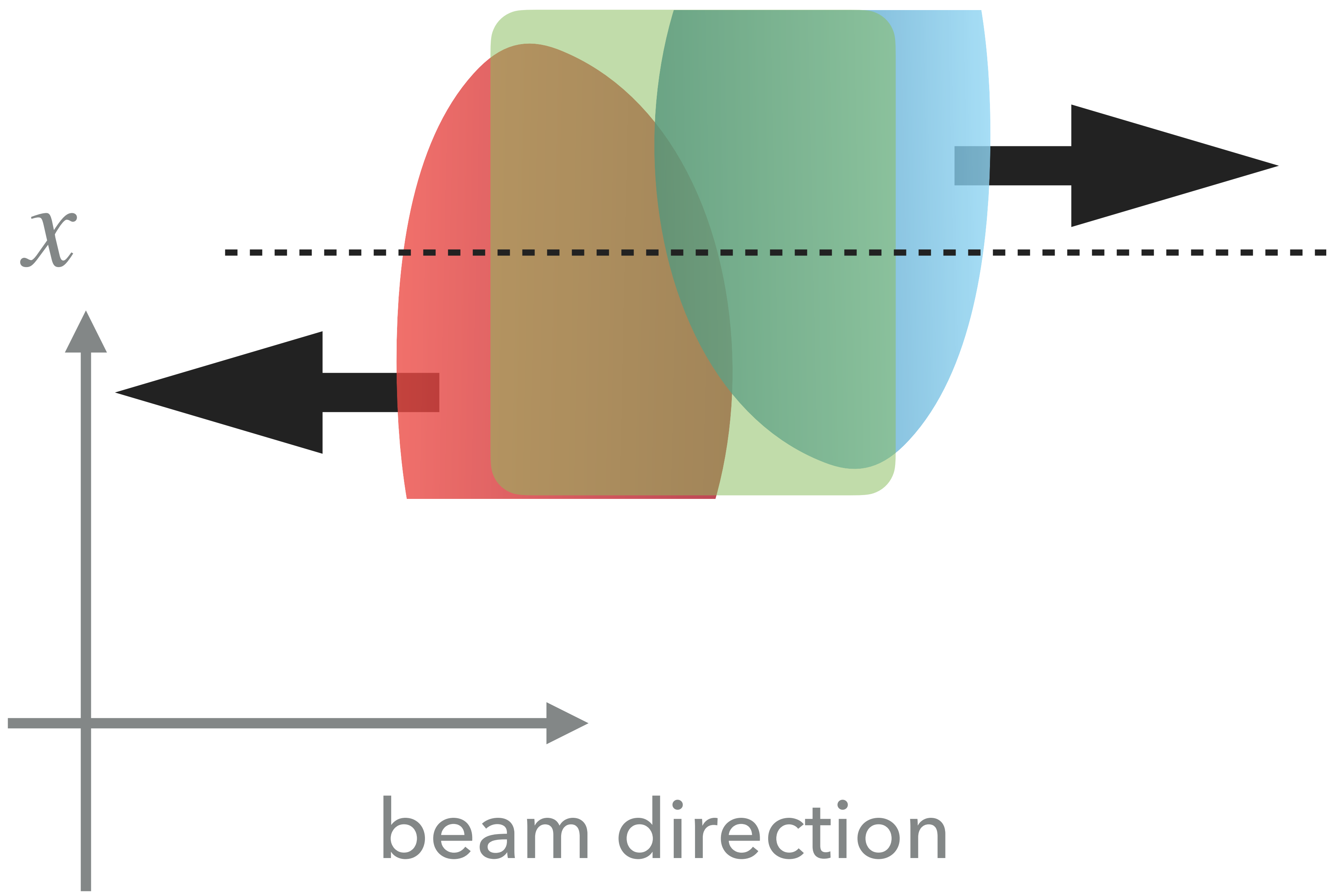

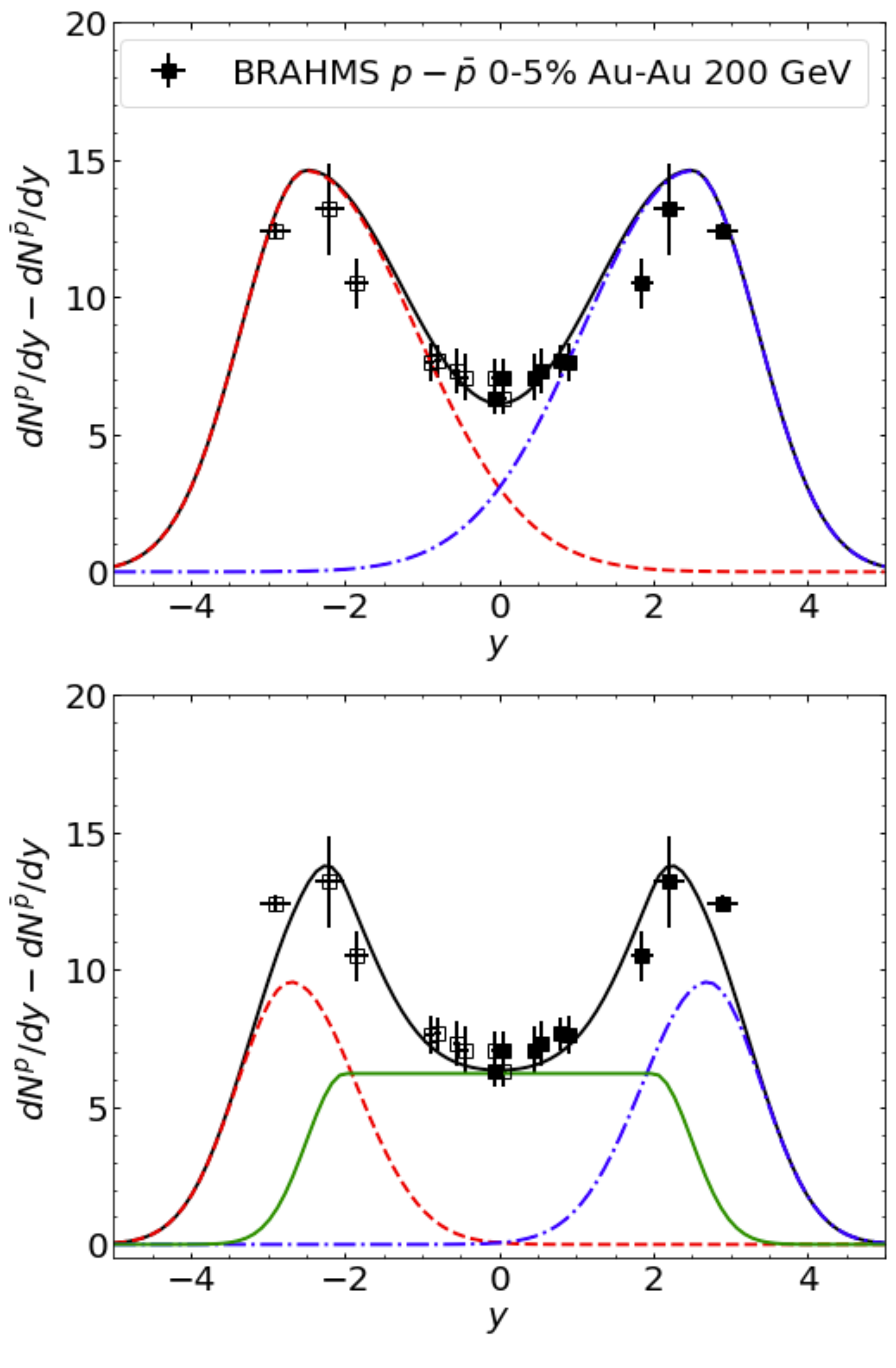

Only for illustration

- To explain the rapidity distributions of net proton yields and baryons' directed flows simultaneously, a plateau component is favored

String junction: Kharzeev, PLB 378, 238 (1996); Sjostrand & Skands, NPB 659, 243 (2003)

DIRECTED FLOW OF BARYONS AT 200 AND 62.4 GEV

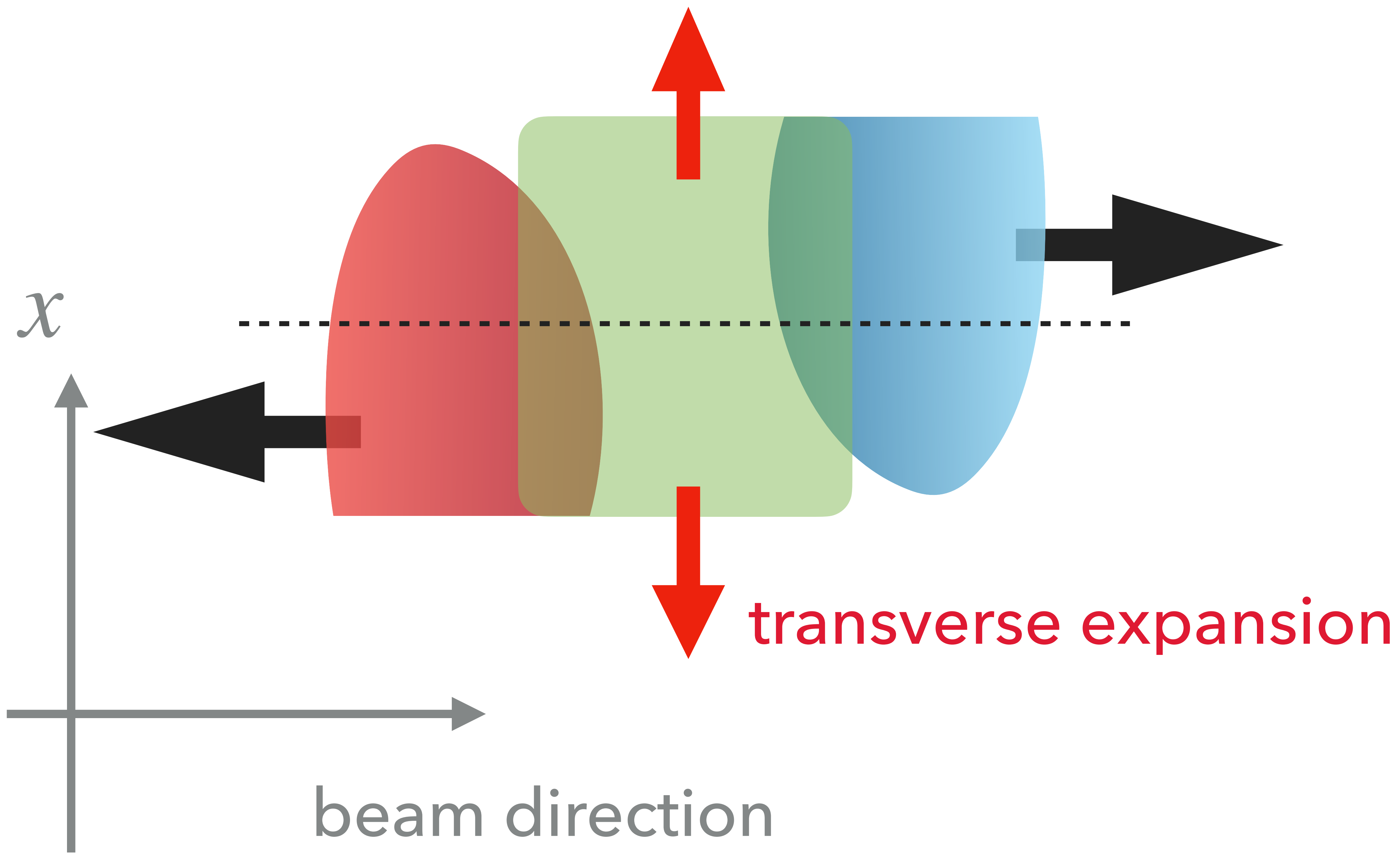

LD, C. Shen, S. Jeon & C. Gale, PRC 108 (2023) L041901

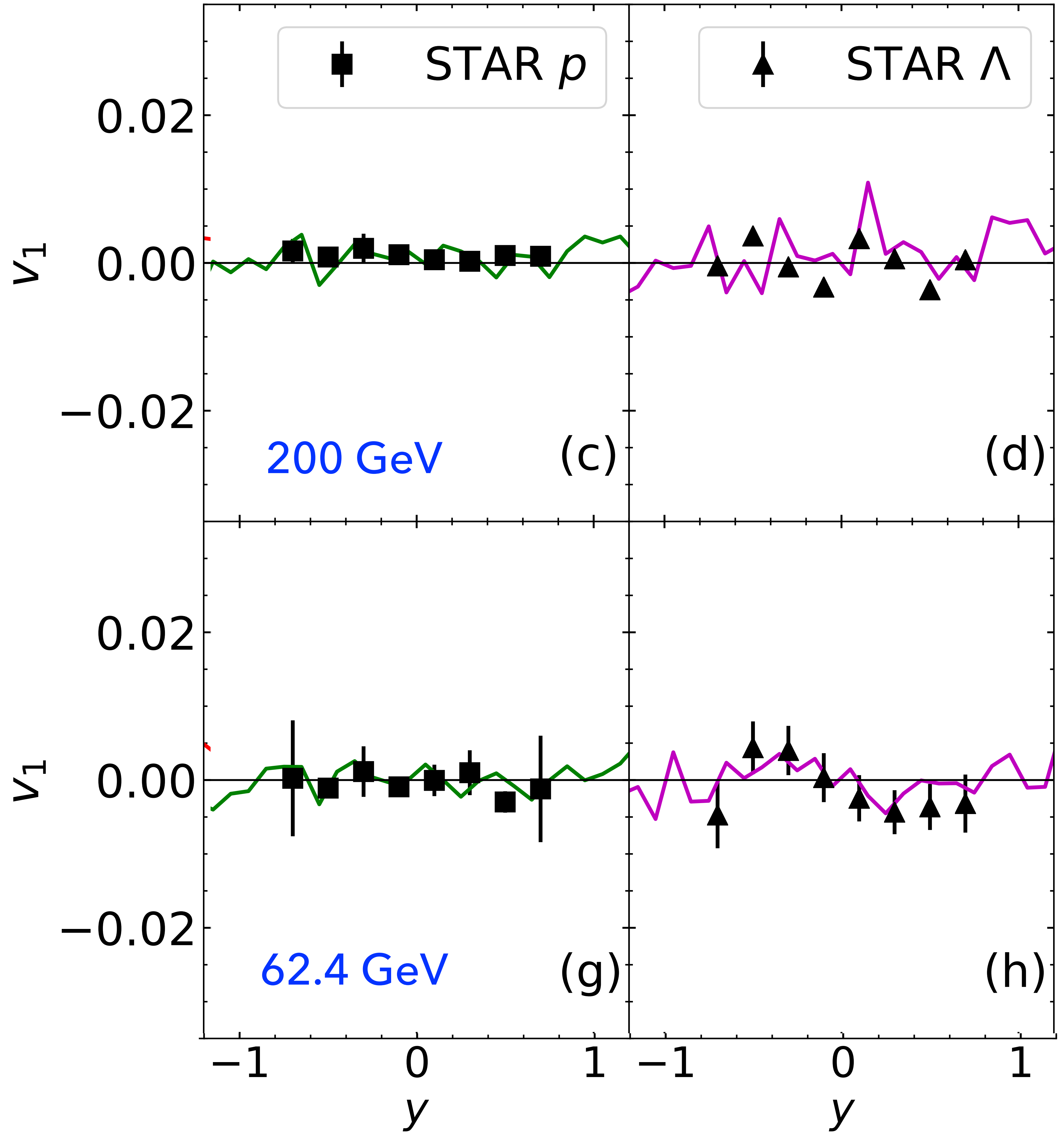

- At high beam energies with large beam rapidities, the plateau dominates around mid-rapidity and strongly reduces baryons' $v_1(y)$.

Data: STAR, PRL 112, 162301 (2014); PRL 120, 062301 (2018)

DIRECTED FLOW OF BARYONS AT 19.6 GEV

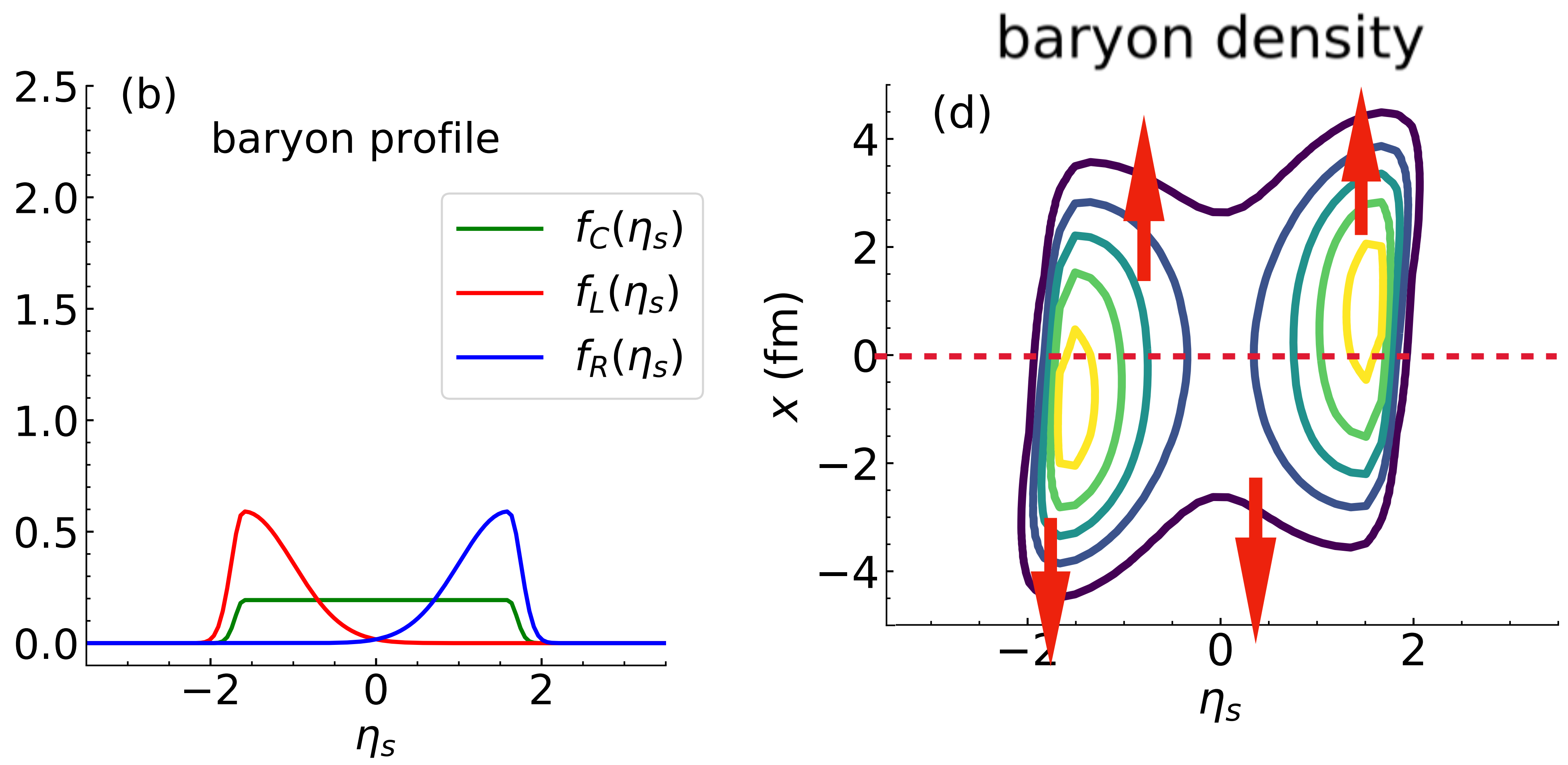

Initial baryon distributions in the reaction plane for 10-40% Au+Au@19.6 GeV

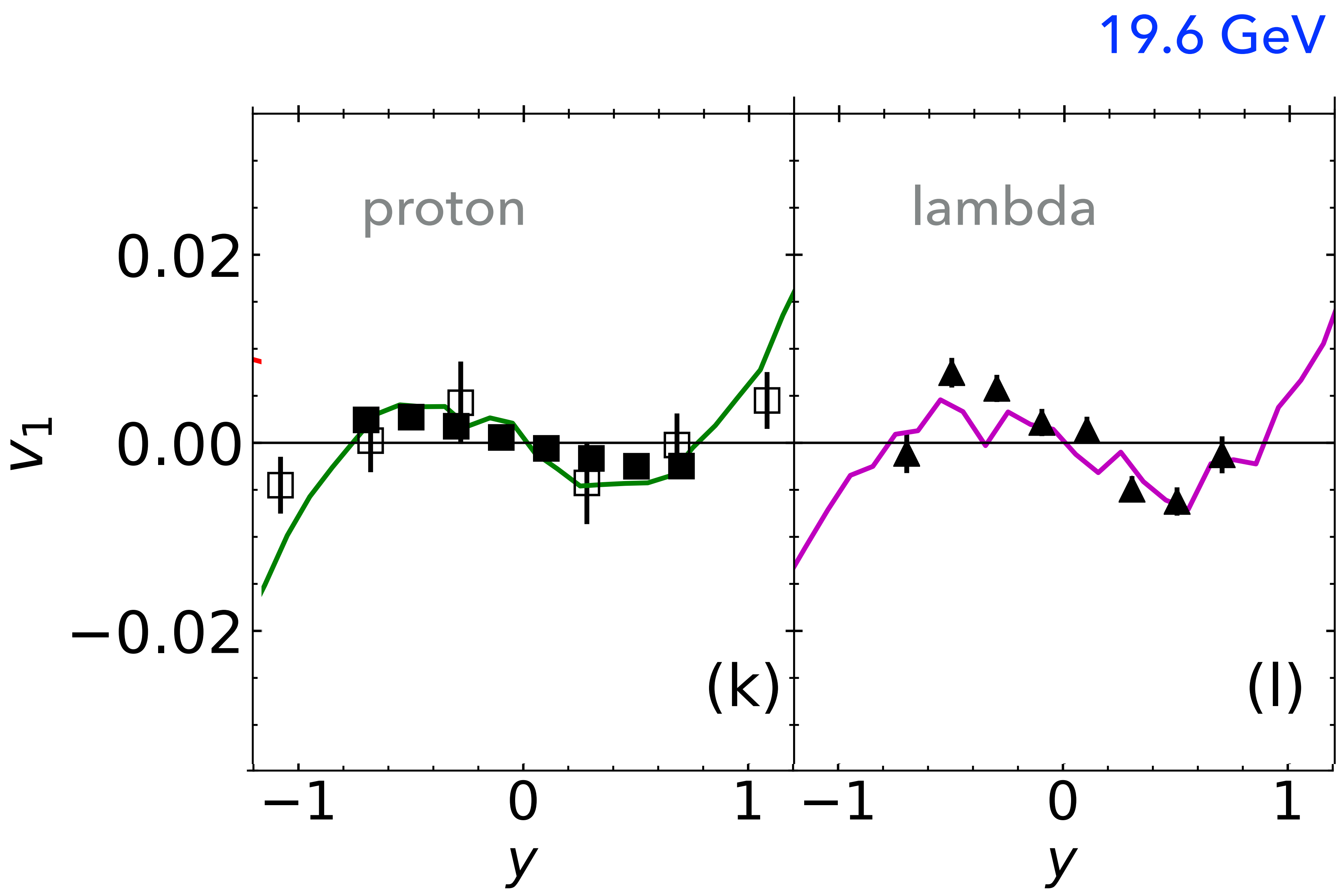

LD, C. Shen, S. Jeon & C. Gale, PRC 108 (2023) L041901

- Transverse expansion + asymmetric distribution of baryon density along x $\Longrightarrow$ double sign change in the slope of $v_1(y)$ for baryons at 19.6 GeV, and positive slope at 7.7 GeV
- The sign change of $dv_1(y)/dy\,|_{y=0}$ is naturally reproduced without a 1st-order phase transition.

DIRECTED FLOW OF BARYONS AT 19.6 GEV

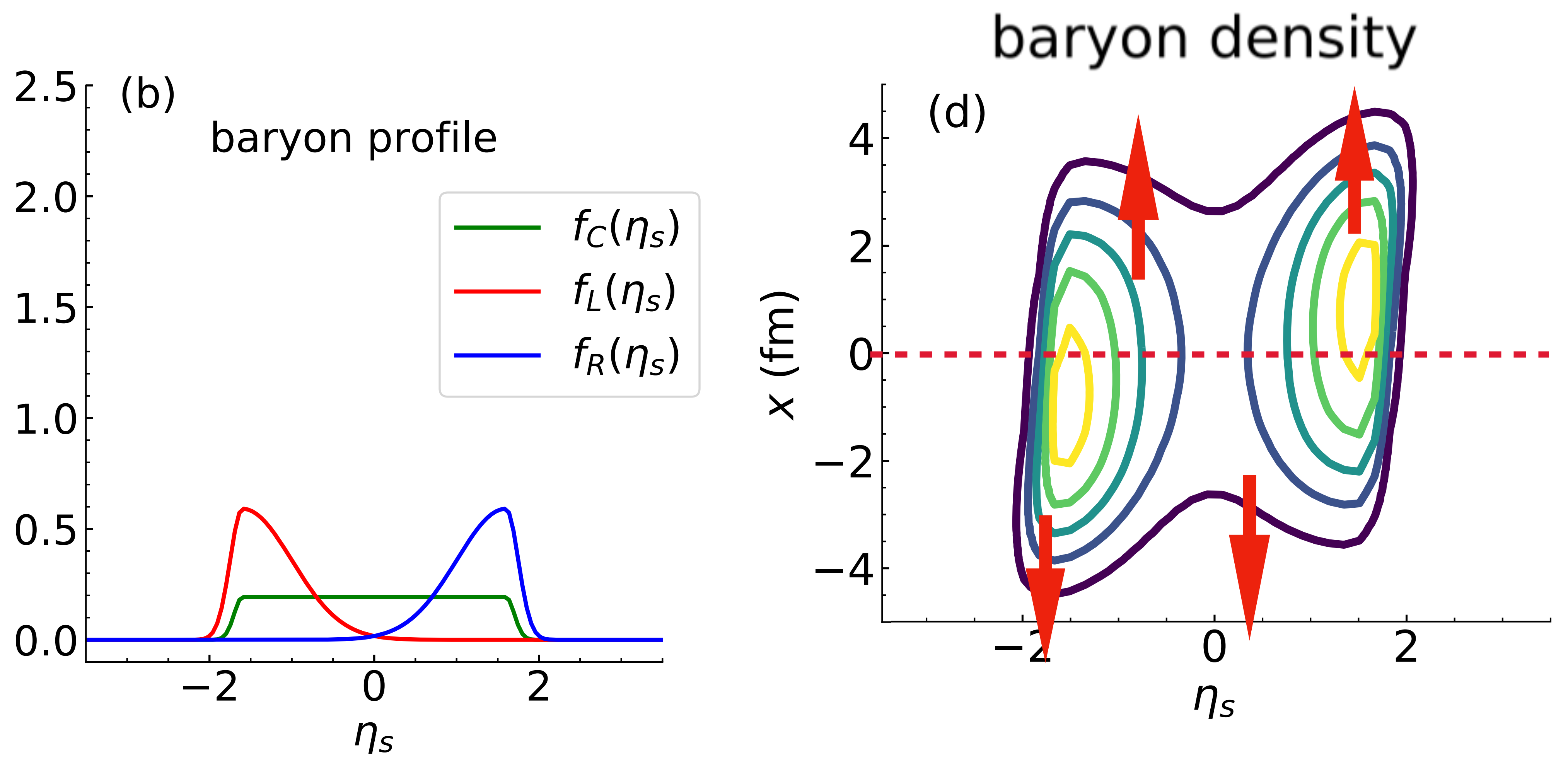

Initial baryon distributions in the reaction plane for 10-40% Au+Au@19.6 GeV

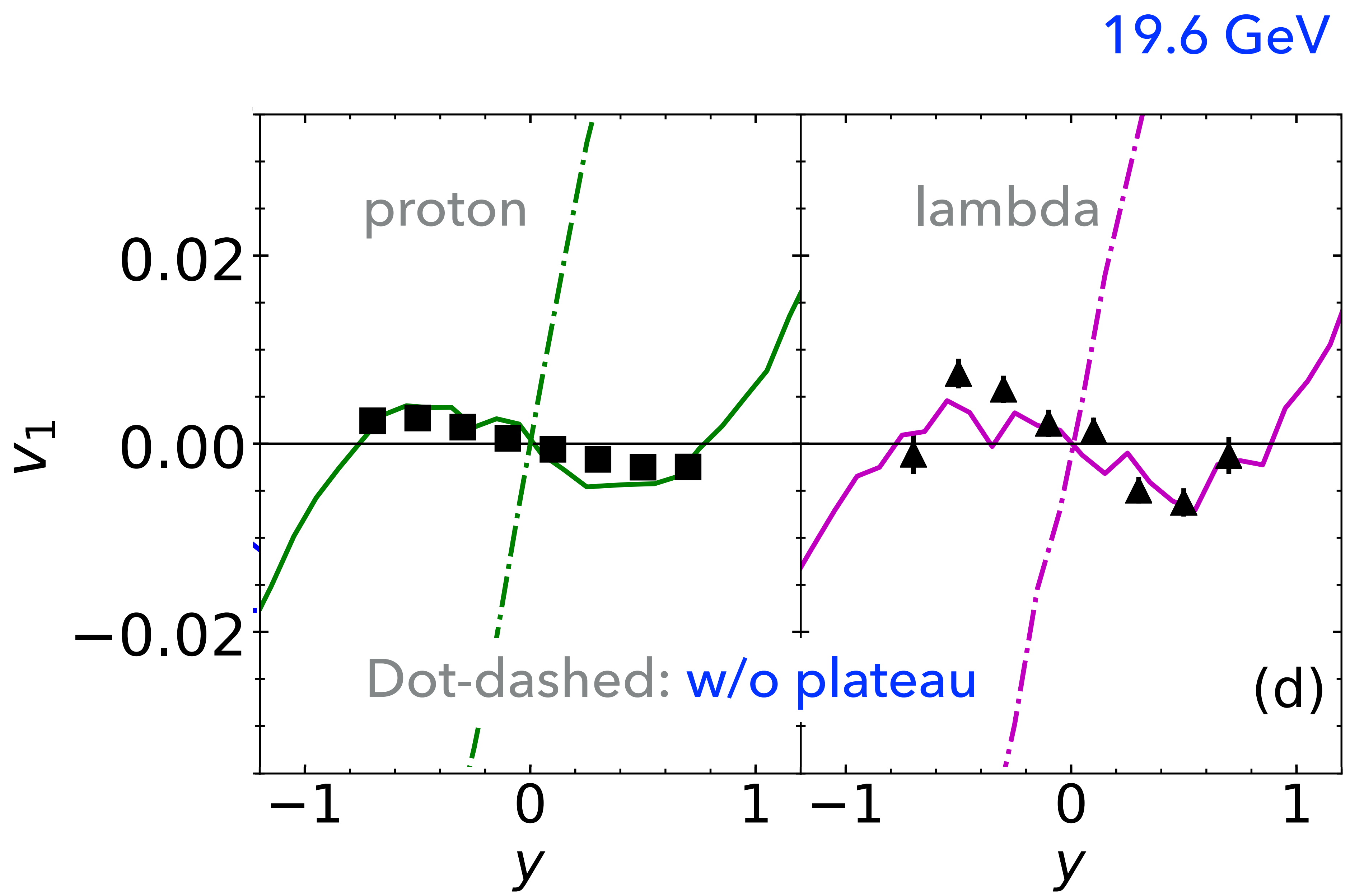

LD, C. Shen, S. Jeon & C. Gale, PRC 108 (2023) L041901

- Transverse expansion + asymmetric distribution of baryon density along x $\Longrightarrow$ double sign change in the slope of $v_1(y)$ for baryons at 19.6 GeV, and positive slope at 7.7 GeV

- The sign change of $dv_1(y)/dy\,|_{y=0}$ is naturally reproduced without a 1st-order phase transition.

DIRECTED FLOW OF BARYONS AT 7.7 GEV

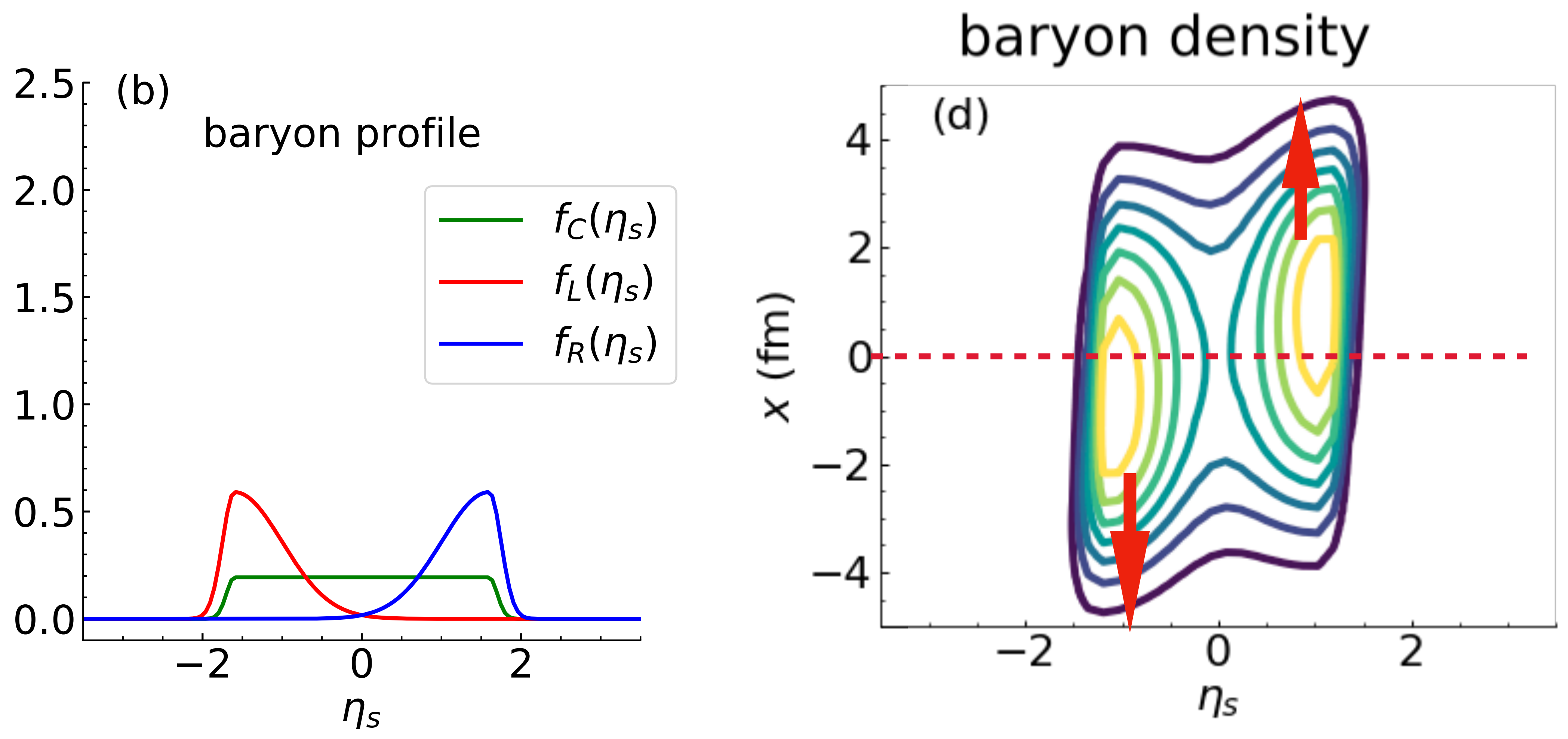

Initial baryon distributions in the reaction plane for 10-40% Au+Au@7.7 GeV

7.7 GeV

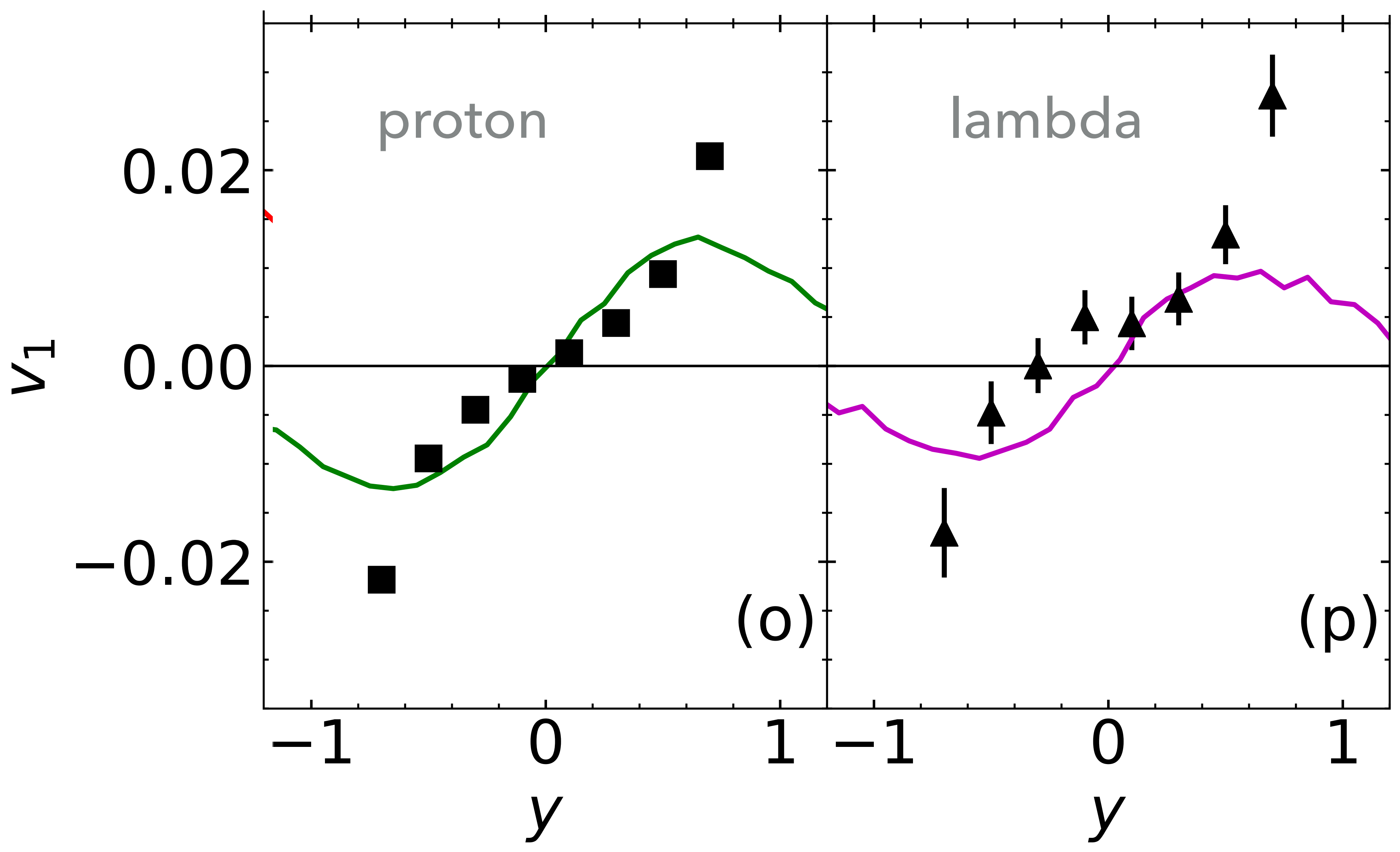

LD, C. Shen, S. Jeon & C. Gale, PRC 108 (2023) L041901

- Transverse expansion + asymmetric distribution of baryon density along x $\Longrightarrow$ double sign change in the slope of $v_1(y)$ for baryons at 19.6 GeV, and positive slope at 7.7 GeV
- The sign change of $dv_1(y)/dy\,|_{y=0}$ is naturally reproduced without a 1st-order phase transition.

PROBING EOS AT FINITE CHEMICAL POTENTIALS

NEOS: Monnai et al, PRC 100, 024907 (2019)

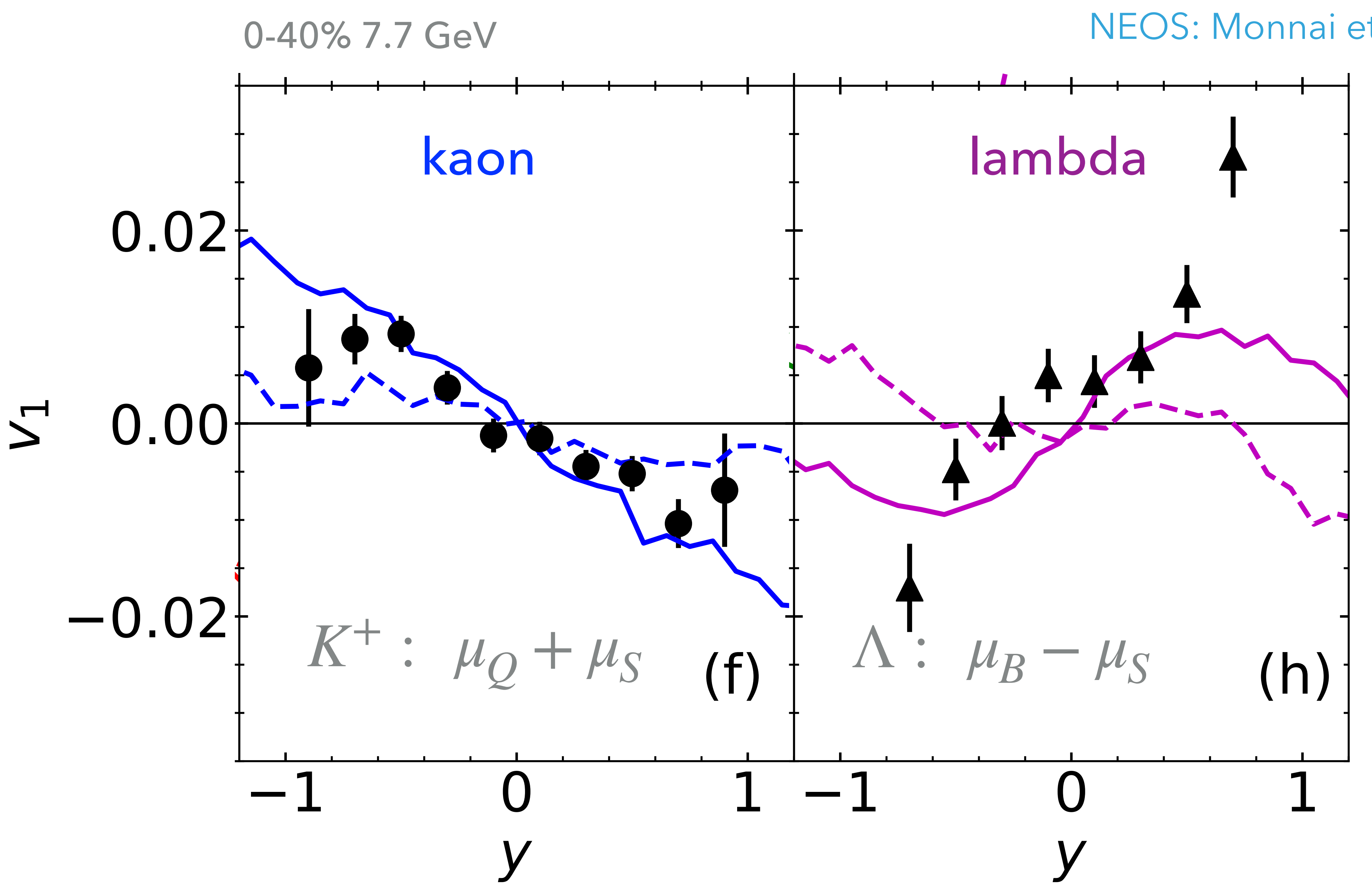

LD, C. Shen, S. Jeon & C. Gale, PRC 108 (2023) L041901

Dashed: NEOS-BQS

Solid: NEOS-B

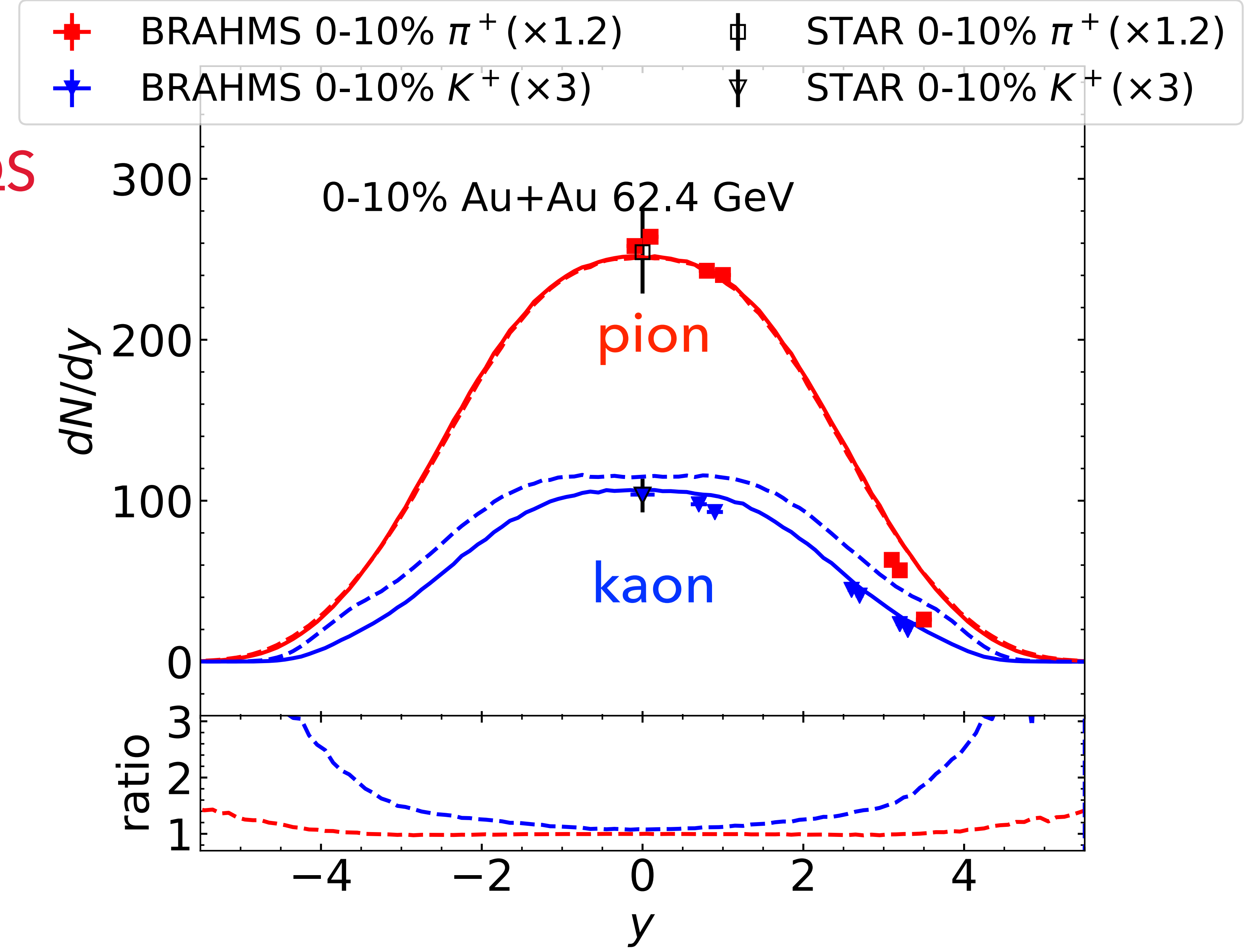

Lipei Du, arXiv: 2401.00596

- Two limits of EoS: NEOS-B, $\mu_S = \mu_Q = 0$ and NEOS-BQS, $n_S = 0, n_Q = 0.4 n_B$ (2D projection of a 4D EOS)
- Rapidity-dependent measurements of identified particles can be used to probe EoS at finite chemical potentials.

ELECTROMAGNETIC PROBES

ELECTROMAGNETIC PROBES

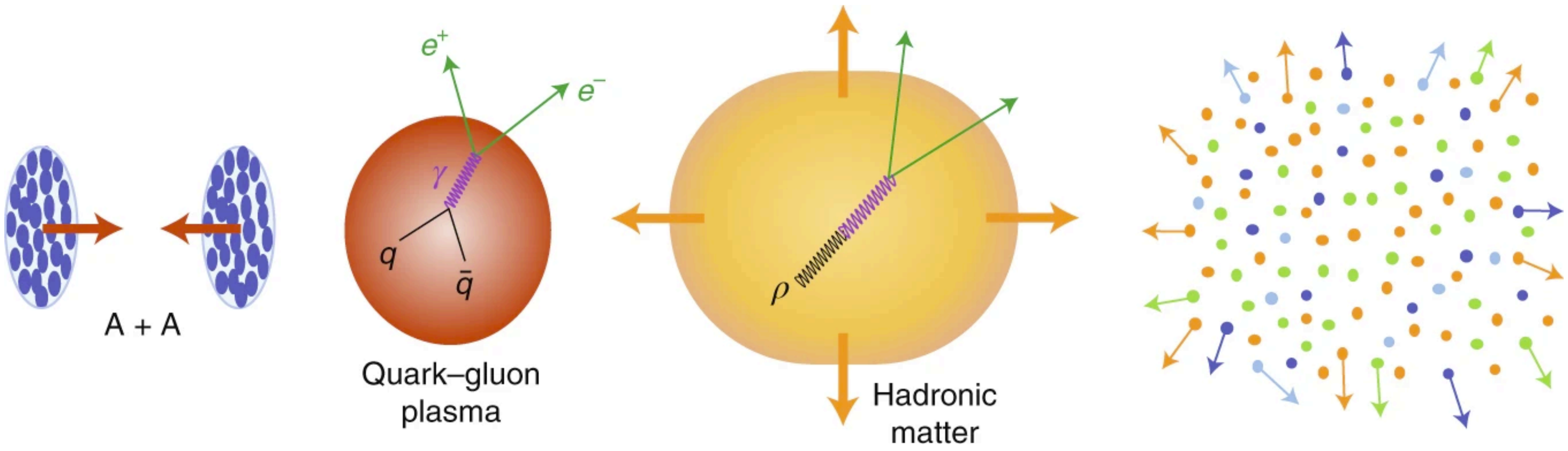

- Electromagnetic probes: dileptons (decay product of virtual photons), real photons
- A penetrating, "clean" probe
  - escape the strongly interacting medium with negligible interactions ("clean")
  - emitted throughout the entire evolution of the medium
- Advantage of dileptons: invariant mass spectrum is not affected by the expansion

DILEPTON SPECTRA

- High-mass region (HMR)
  - Drell-Yan process

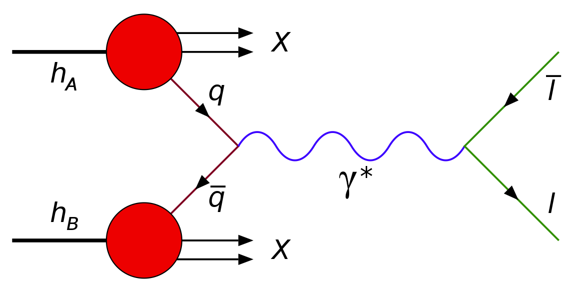

  - decays of J/ψ
- Intermediate-mass region (IMR)
  - thermal emission from QGP

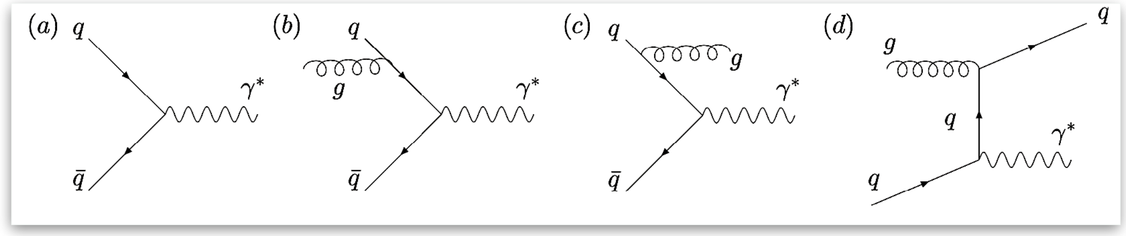

  - semileptonic decays from open heavy flavor-antiflavor pair, e.g. $D/\bar{D}$
- Low-mass region (LMR)
  - thermal emission from hadronic matter
  - direct decays of $\rho/\omega/\phi$ (ρ is short-lived)
  - Dalitz (three body) decays of $\pi^0/\eta/\eta'$

Dilepton cocktail: late decays of hadrons

STAR, PLB 750 (2015) 64–71

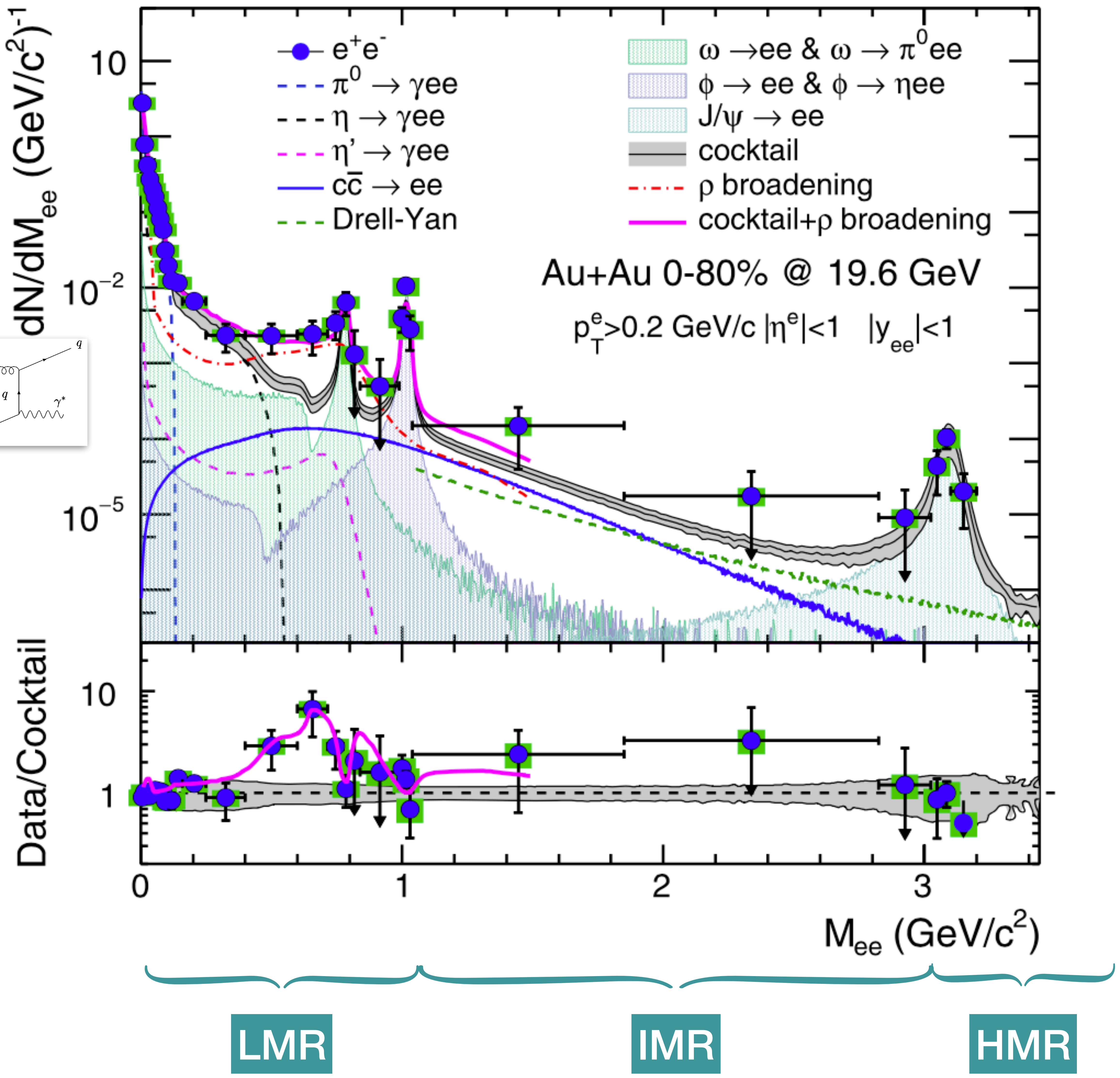

THERMAL DILEPTON PRODUCTION

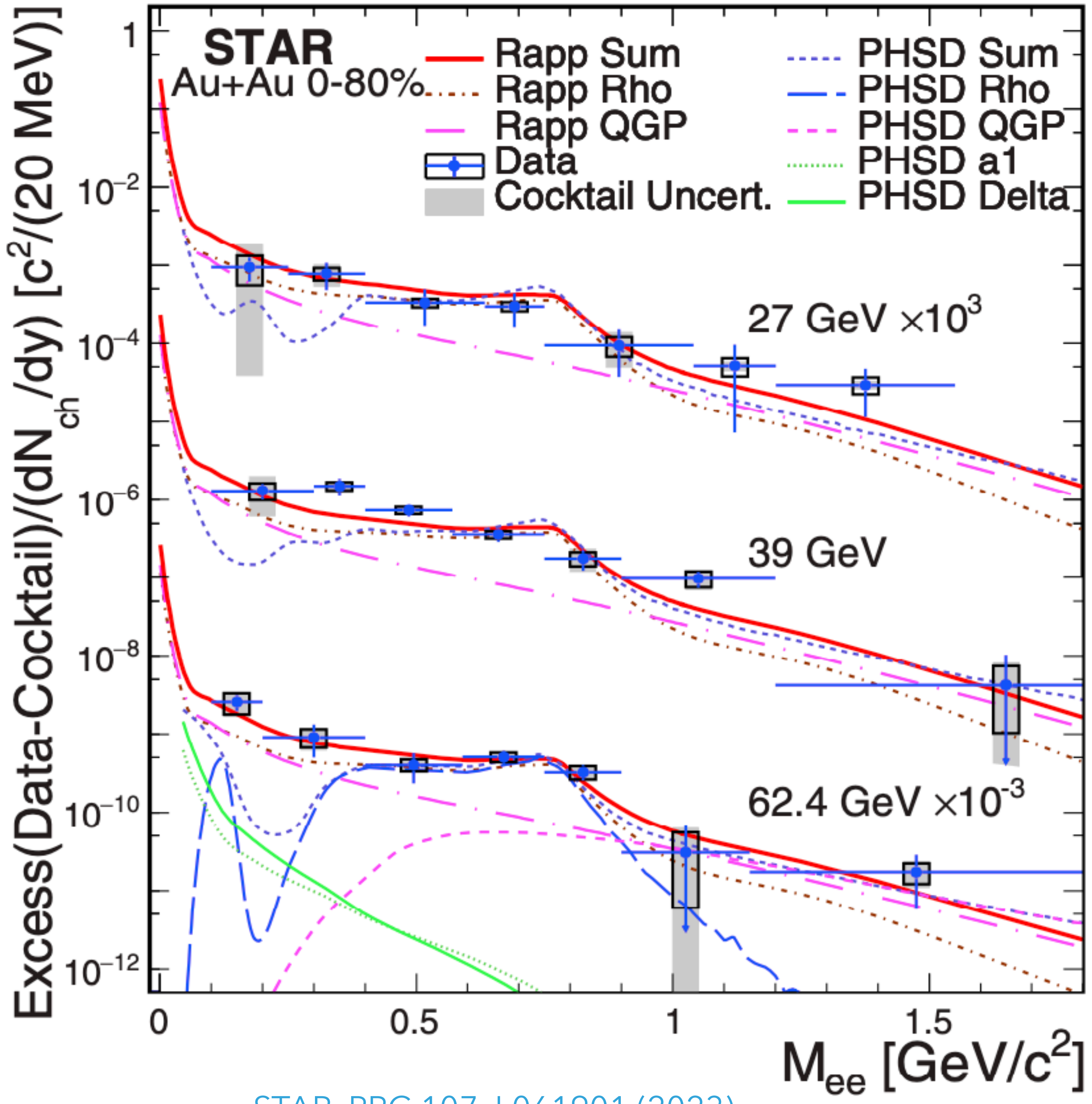

STAR, PRC 107, L061901 (2023)

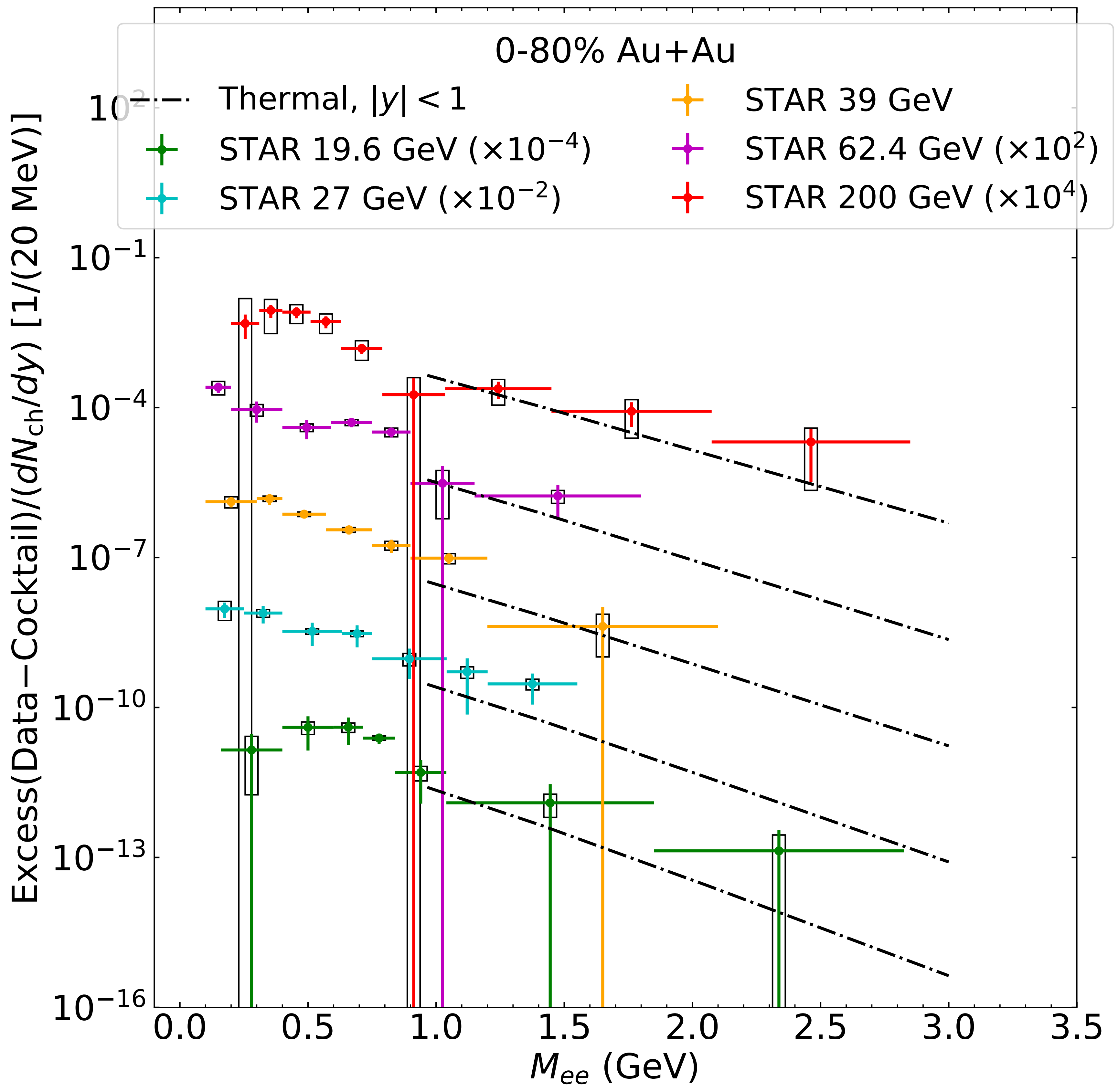

https://github.com/LipeiDu/DileptonEmission

J. Churchill, **LD**, C. Gale, G. Jackson & S. Jeon, PRC 109, 044915 (2024), PRL 132, 172301 (2024)

NA60, PRL 100, 022302 (2008); EPJC 59 607-623 (2009). STAR, PRL113, 022301 (2014); PRC 92, 024912 (2015); PLB 750 (2015) 64-71; PRC 107, L061901 (2023). HADES, Nat. Phys.,1040-1045 (2019).

- First results of NLO dilepton emission at nonzero μ_B with hydrodynamic model

RAPIDITY AND μ_B DEPENDENCE

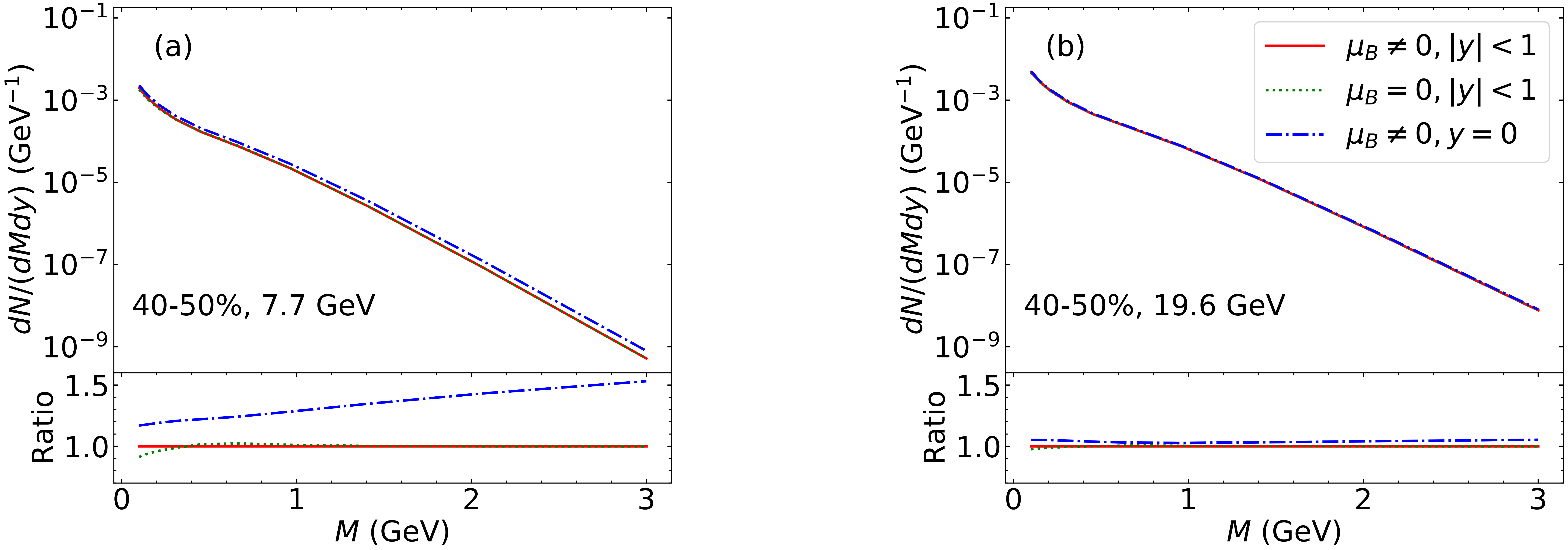

- μ_B-dependence is not significant for 7.7 GeV and higher beam energies
- At 7.7 GeV, a strong boost-non-invariant effect is observed

DILEPTON PRODUCTION IN T AND τ

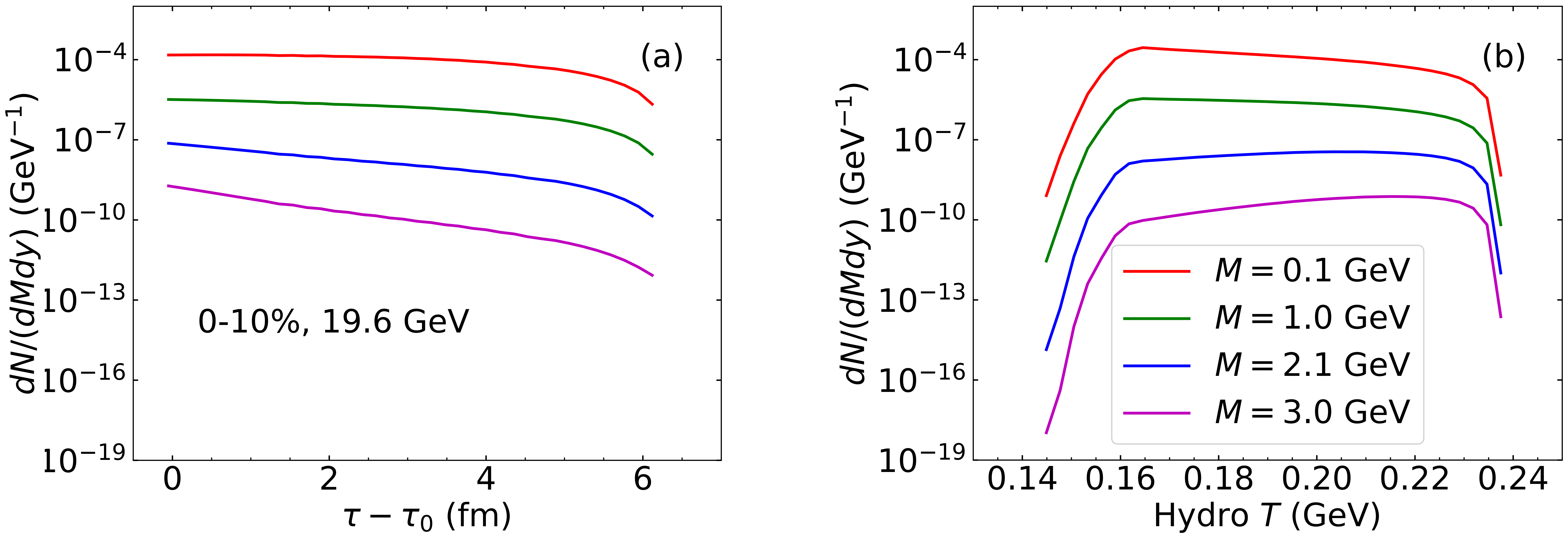

- Two effects at play:
  - The emission rate decreases as the temperature decreases
  - The volume of the system increases with time

TEMPERATURE EXTRACTION

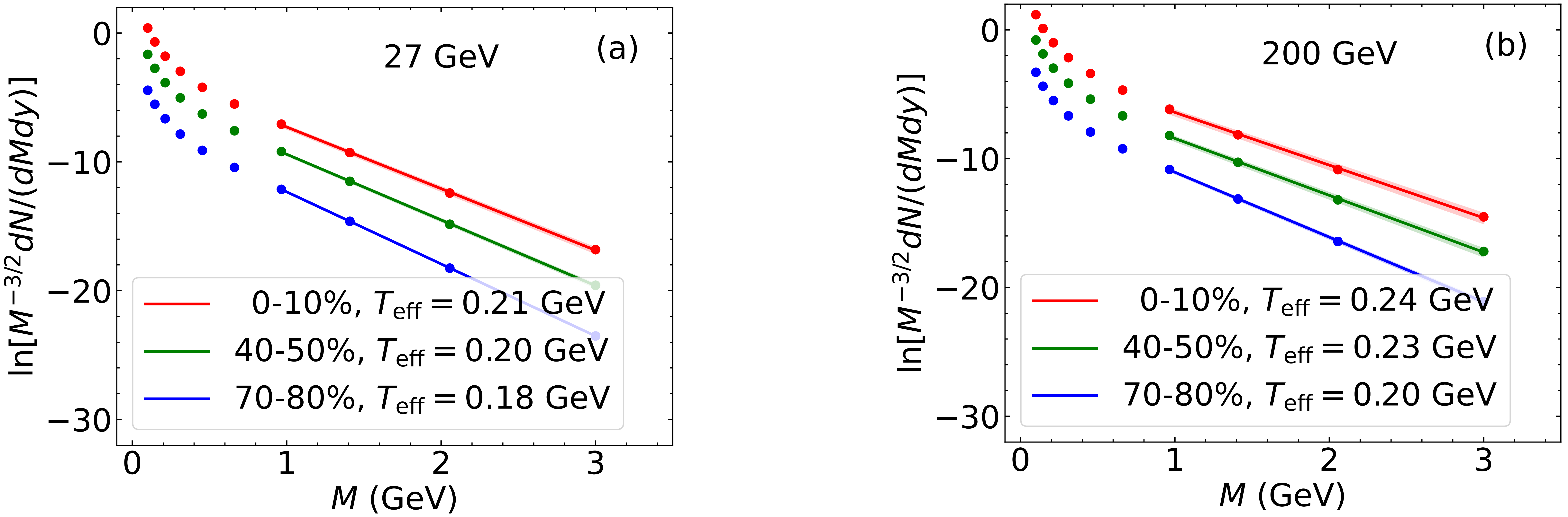

- In non-relativistic approximation ($M \gg T$), the emission rate $\dfrac{dR}{dM} \propto (MT)^{3/2}\mathrm{e}^{-M/T}$
- Thermal dileptons within $1\mathrm{GeV} \lesssim M \lesssim 3\mathrm{GeV}$ for temperature extraction
- Uncertainties are larger at higher beam energies and in central collisions since the fireball has longer lifetimes and thus larger temperature variations

NA60, PRL 100, 022302 (2008); EPJC 59 607-623 (2009). STAR, 2402.01998. HADES, Nat. Phys.,1040–1045 (2019). Rapp and van Hees, PLB 753, 586 (2016)

TEMPERATURE EXTRACTION IN τ

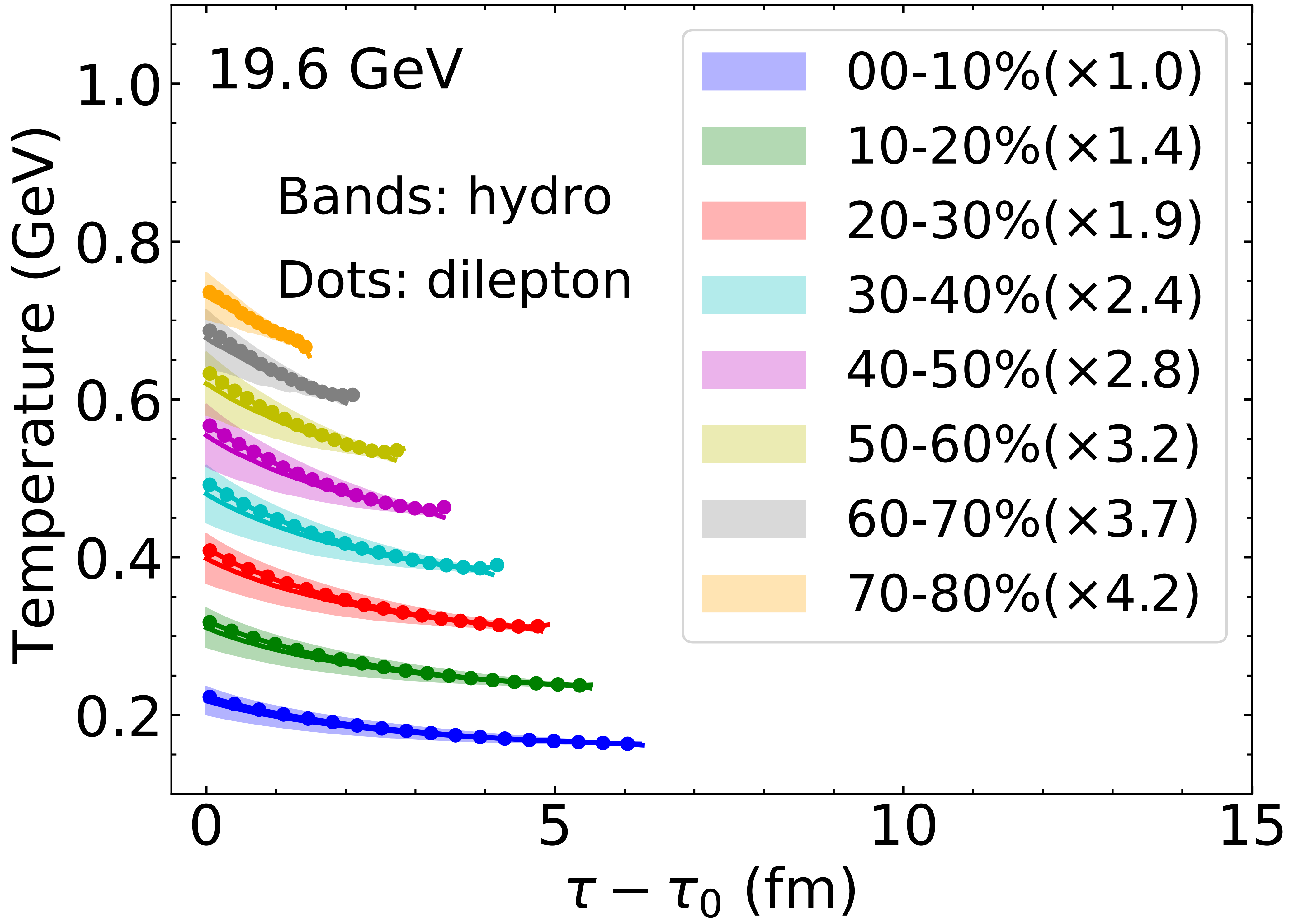

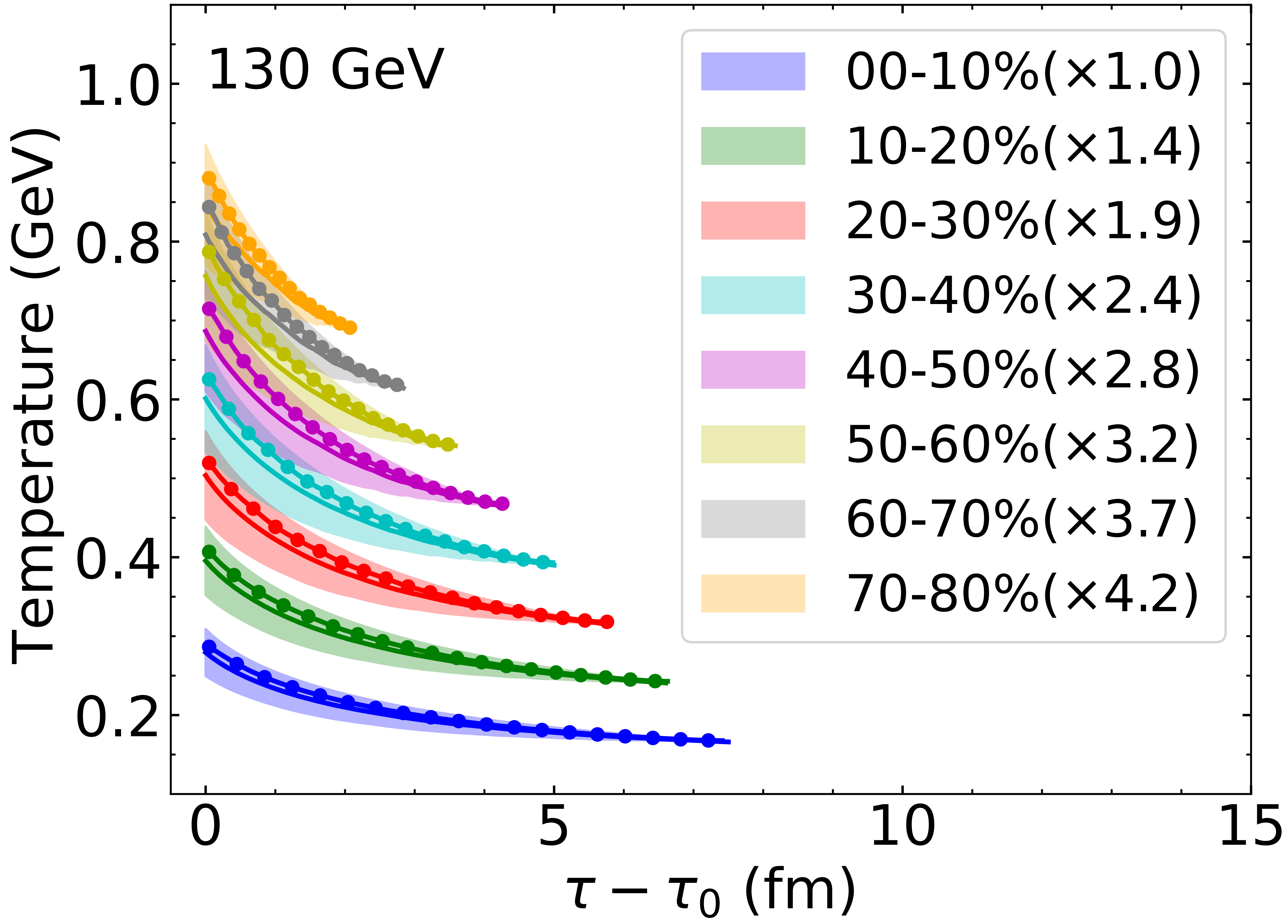

- Curves & bands: hydrodynamic temperature. curve: mean temperature; band: standard deviation
- Dots: effective temperature extracted from dilepton spectra at various time steps

Photon thermometer: Shen, Heinz, Paquet, and Gale, PRC 89, 044910 (2014)

THERMAL DILEPTON AS THERMOMETER

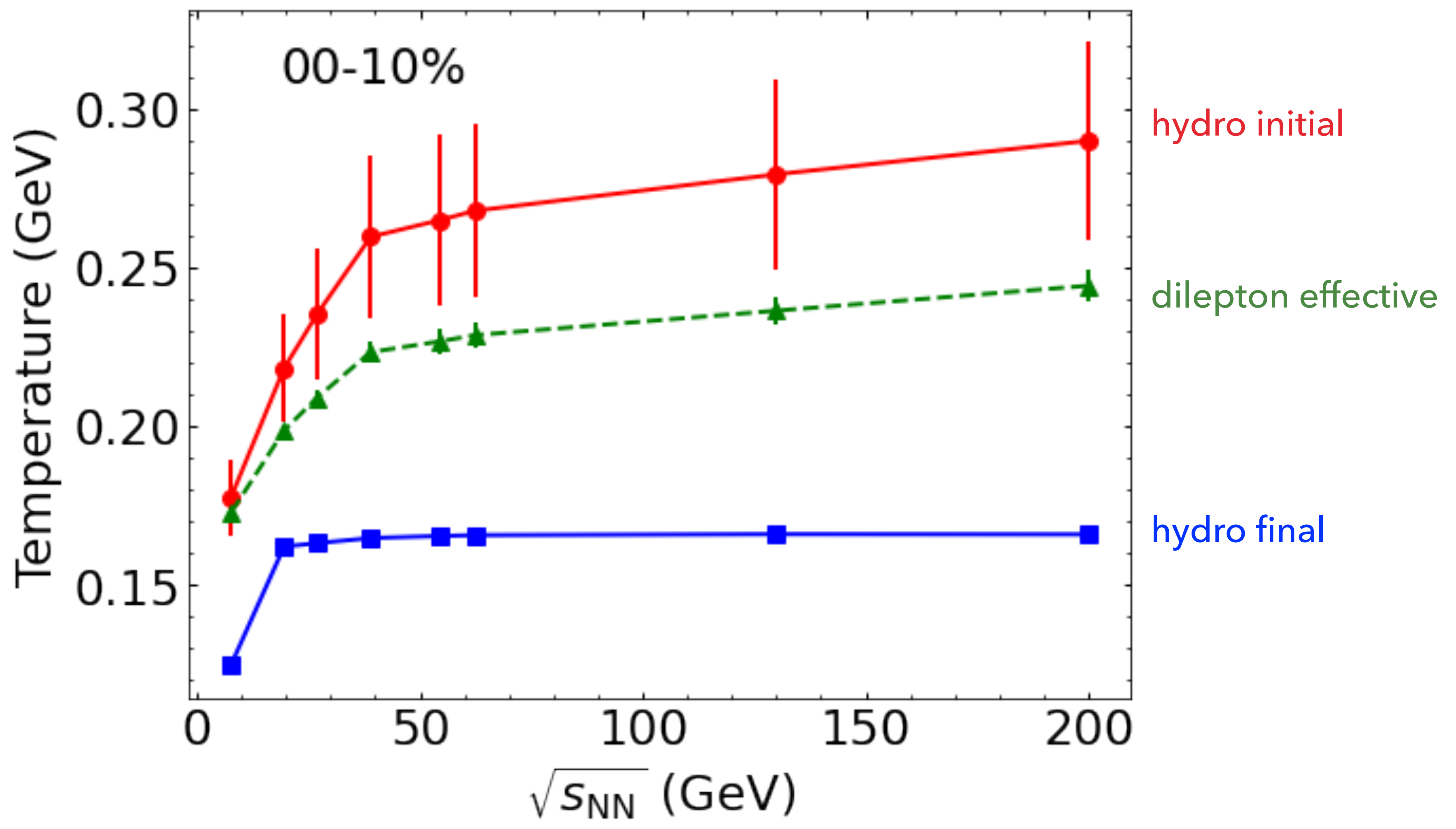

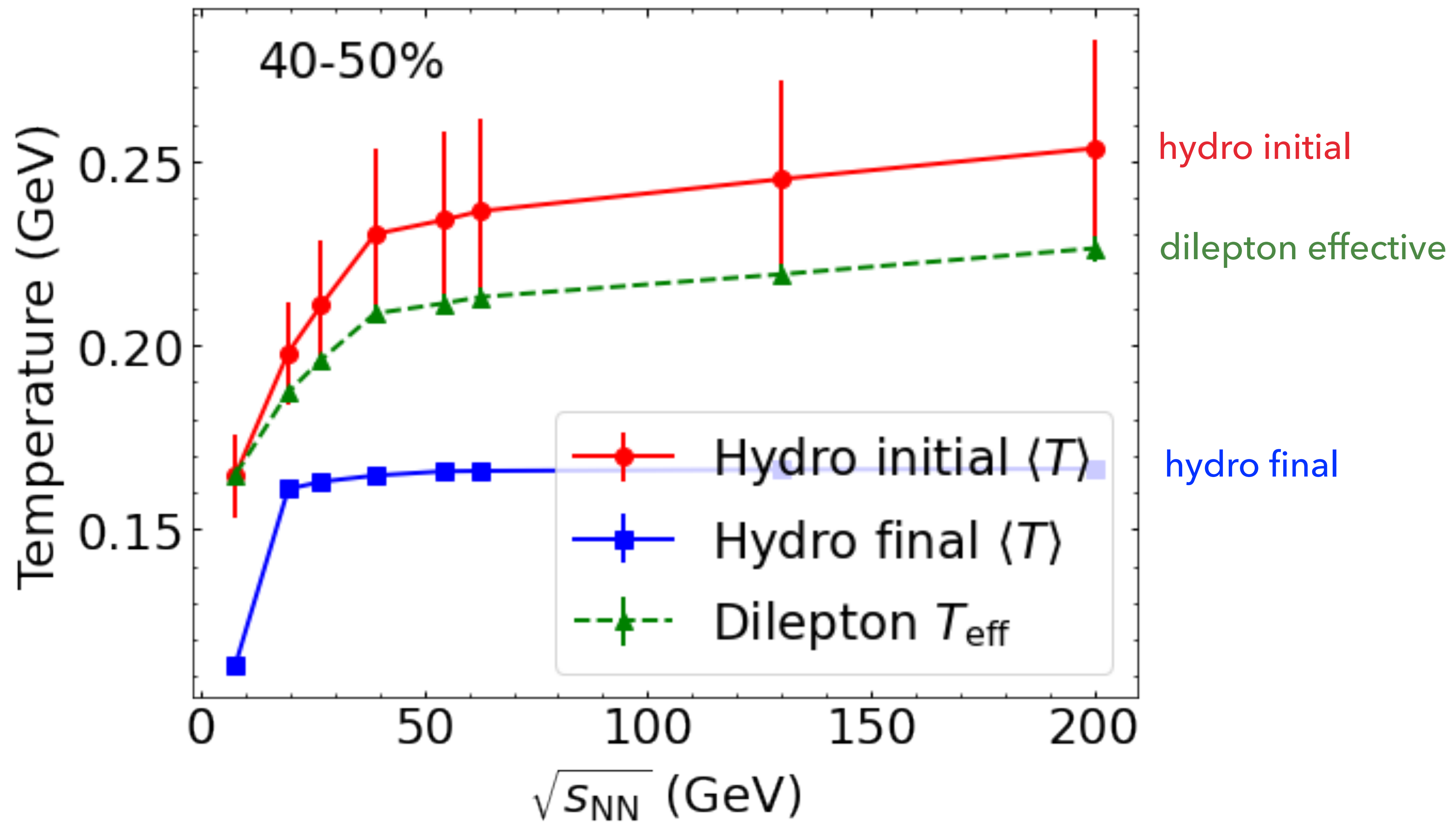

- The final temperature is approximately a constant for $\sqrt{s_{\mathrm{NN}}} \gtrsim 19.6$ GeV and much smaller at $\sqrt{s_{\mathrm{NN}}} = 7.7$ GeV because of the baryon chemical potential
- A correlation between the hydro initial temperature and effective temperature can be observed

Kajantie and Miettinen, Z. Phys. C 9, 341 (1981); Hwa and Kajantie, PRD 32, 1109 (1985); Rapp and van Hees, PLB 753, 586 (2016);

THERMAL DILEPTON AS THERMOMETER

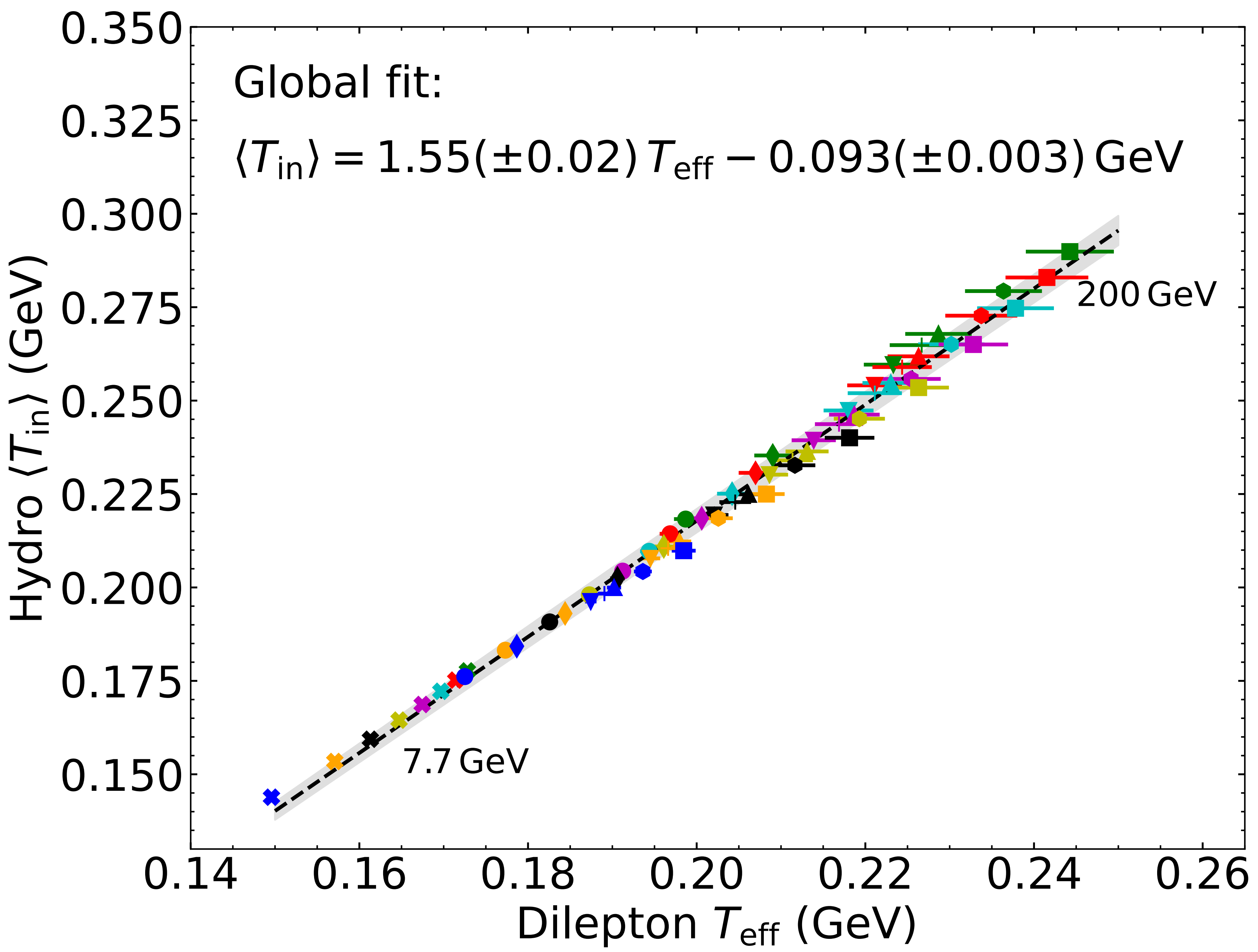

https://github.com/LipeiDu/DileptonEmission

J. Churchill, **LD**, C. Gale, G. Jackson & S. Jeon, PRC 109, 044915 (2024), PRL 132, 172301 (2024)

- Combining all energies and centralities, a strong correlation is observed between the initial hydro temperature and the effective temperature extracted from the dilepton spectra
- Measure the temperature of the evolving QCD fireball in a way that is unaffected by dynamical distortions

Kajantie and Miettinen, Z. Phys. C 9, 341 (1981); Hwa and Kajantie, PRD 32, 1109 (1985); Rapp and van Hees, PLB 753, 586 (2016);

SUMMARY AND OUTLOOK

SUMMARY AND OUTLOOK

- Summary:
  - Considering rapidity-variation in thermodynamic properties is essential at BES.
  - The first results were shown for dilepton emission at NLO and finite baryon chemical potential in a hydrodynamical model.
  - Dileptons can measure the temperature of the evolving QCD fireball in a way that is unaffected by dynamic distortions.
- Outlook:
  - Constraining the longitudinal properties with limited rapidity data
  - More quantitative and systematic studies on multi-messenger heavy-ion collision physics

A THEORY OVERVIEW

Chapter 1

The QCD phase diagram and Beam Energy Scan physics: a theory overview

Lipei Du,[1,2*] Agnieszka Sorensen,[3†] and Mikhail Stephanov[4,5‡]

[1]*Department of Physics, McGill University, Montreal, Quebec H3A 2T8, Canada*

[2]*Nuclear Science Division, Lawrence Berkeley National Laboratory, Berkeley, CA 94270, USA*

[3]*Institute for Nuclear Theory, University of Washington, Seattle, WA 98195, USA*

[4]*Department of Physics and Laboratory for Quantum Theory at the Extremes, University of Illinois, Chicago, IL 60607, USA*

[5]*Kadanoff Center for Theoretical Physics, University of Chicago, Chicago, Illinois 60637, USA*

L. Du, A. Sorensen, and M. Stephanov, 2402.10183 (a contribution to Quark-Gluon Plasma 6)

THANK YOU FOR YOUR ATTENTION!

NEW PARAMETRIC BARYON INITIAL CONDITION

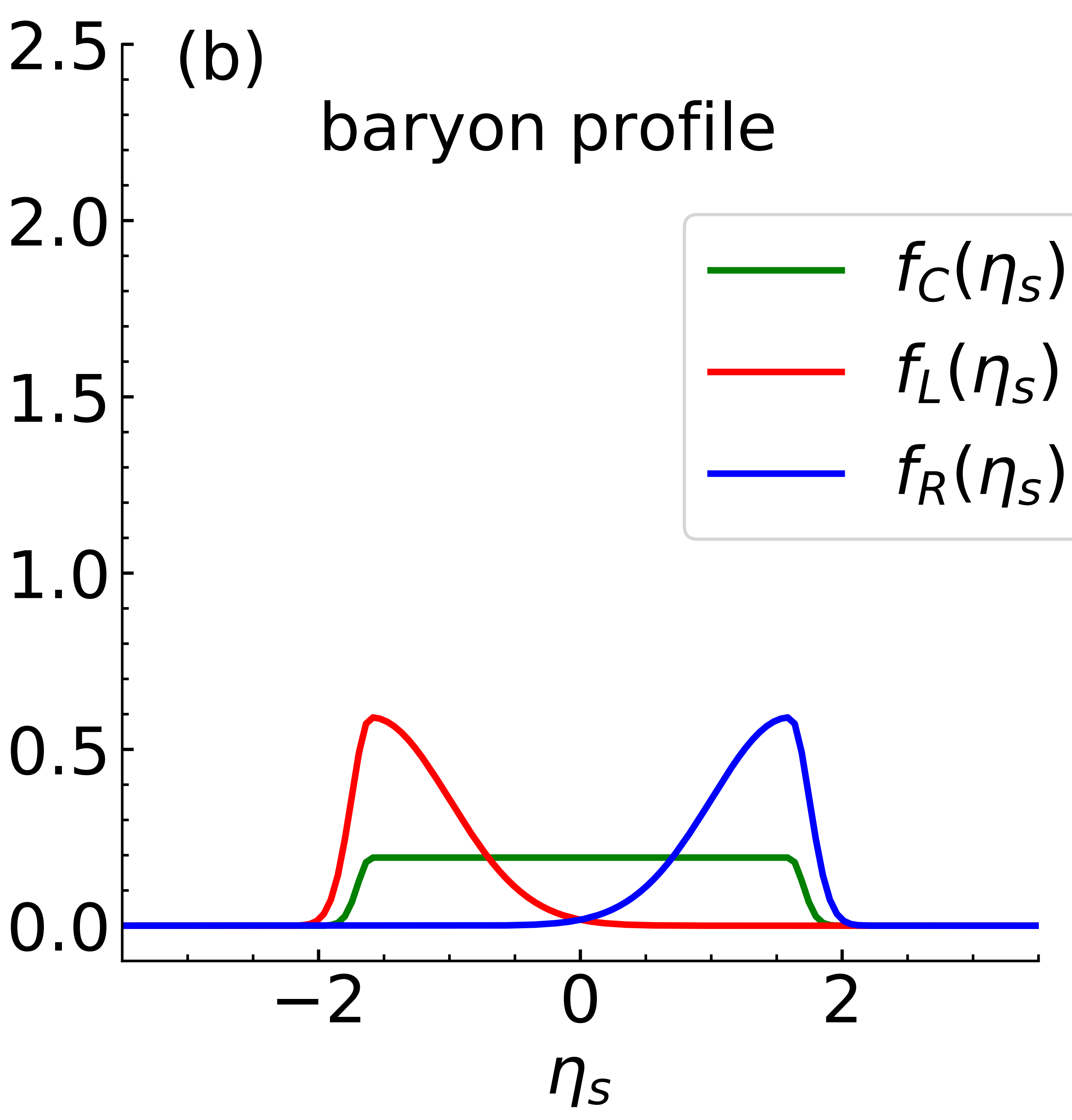

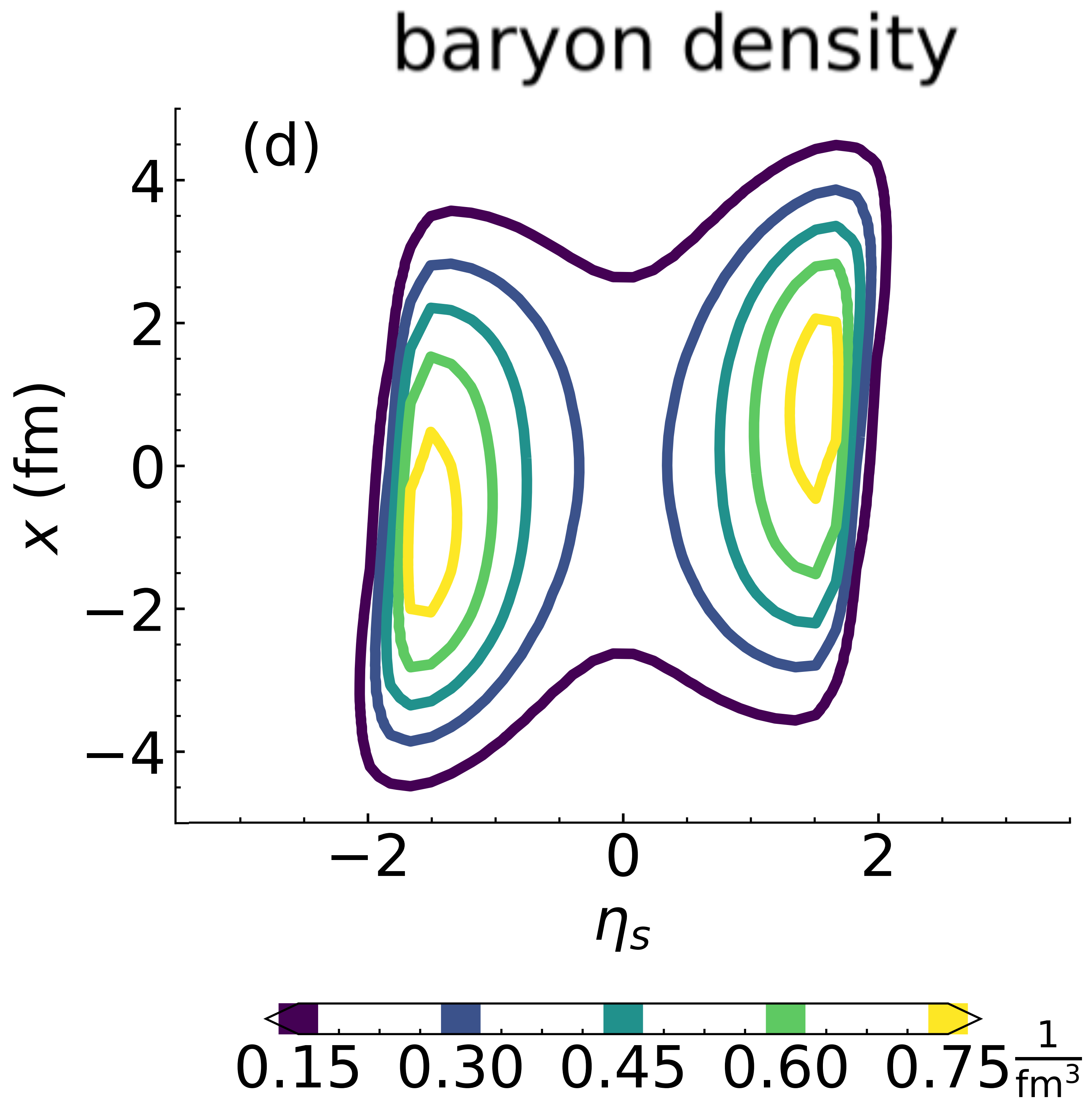

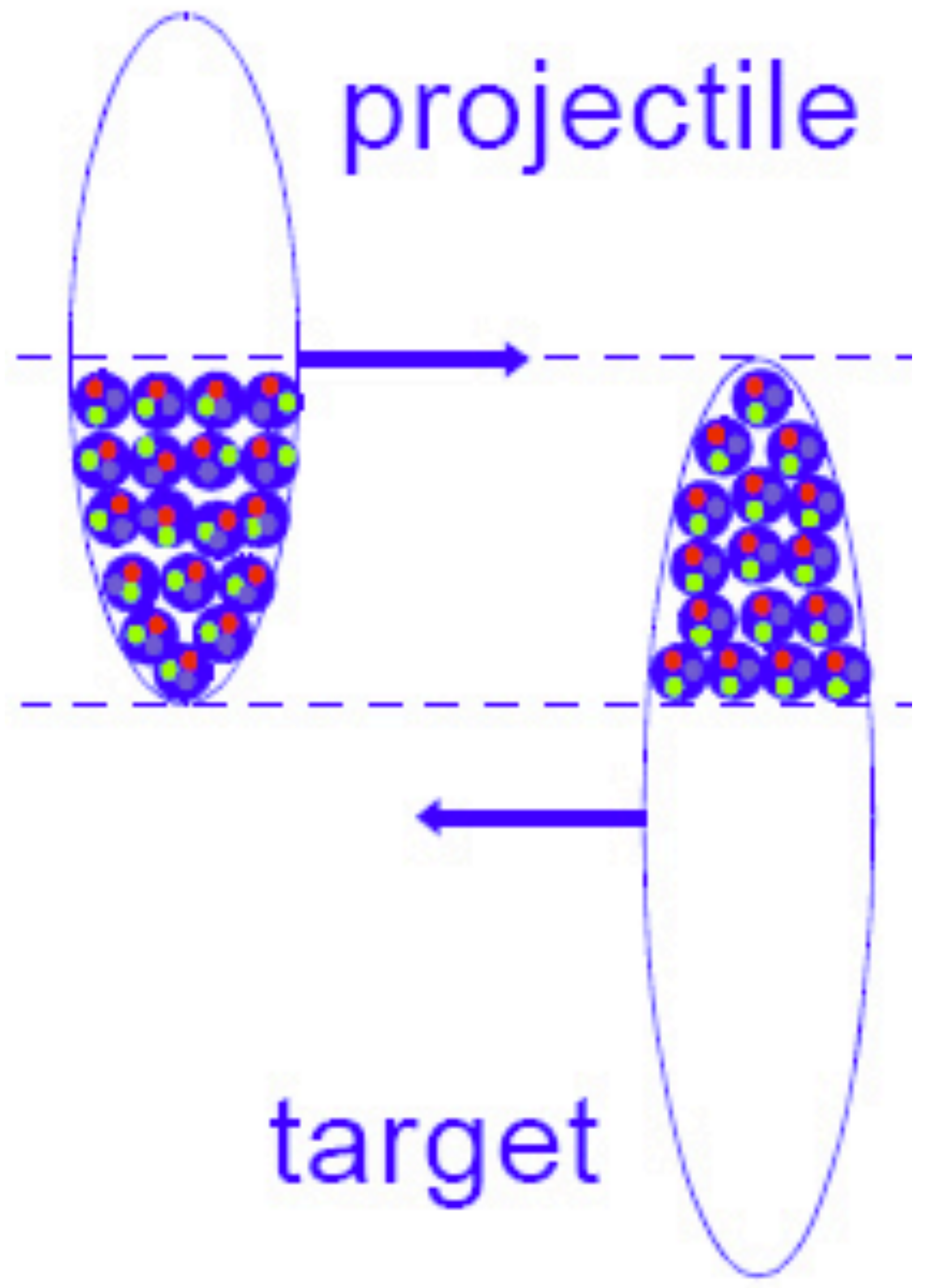

- A rapidity-independent "plateau" component in initial baryon profile & tilted baryon peaks describing the varying baryon stopping in the transverse plane

LD, C. Shen, S. Jeon & C. Gale, PRC 108 (2023) L041901

APPLICATION OF PERTURBATIVE QCD

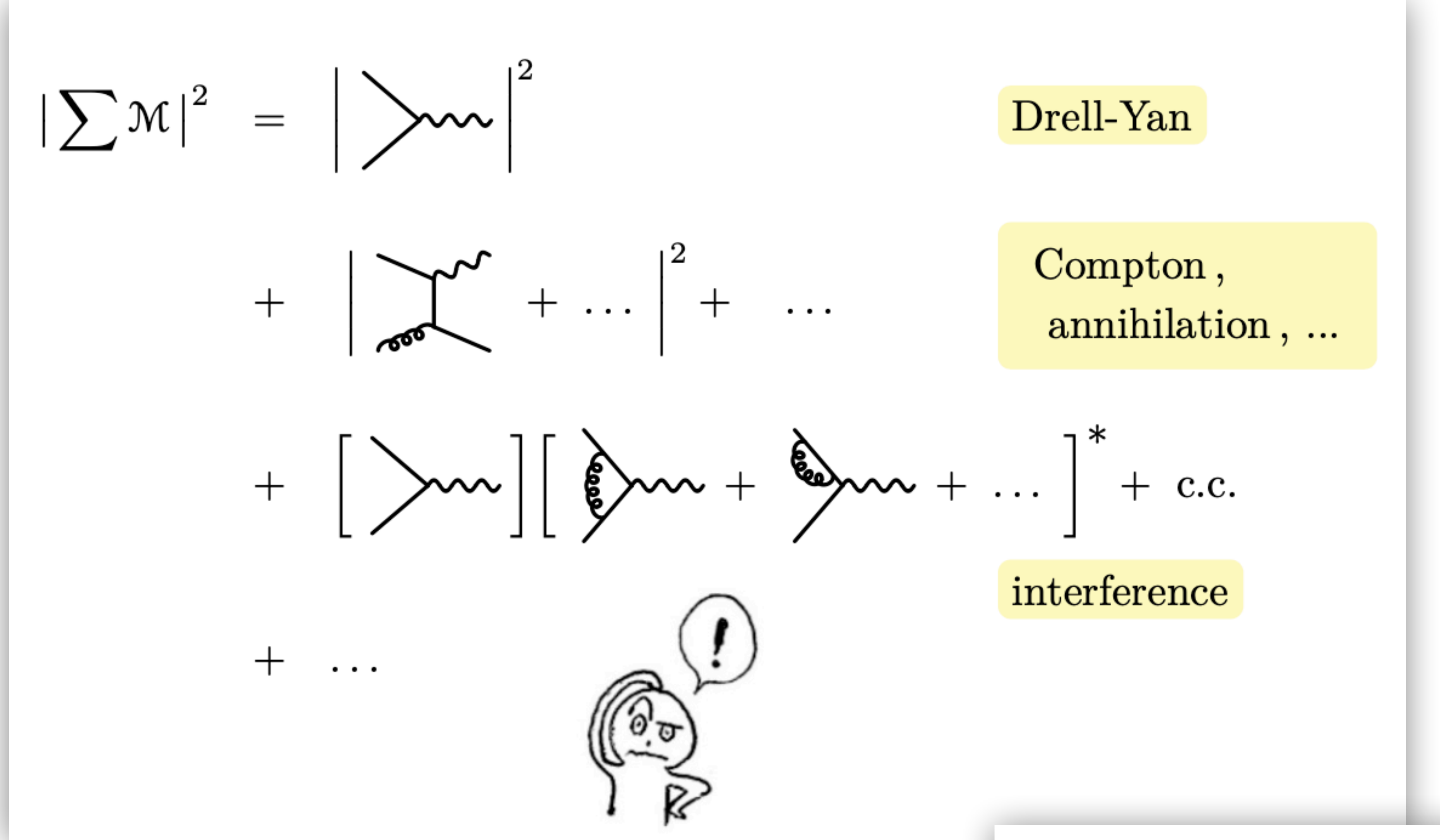

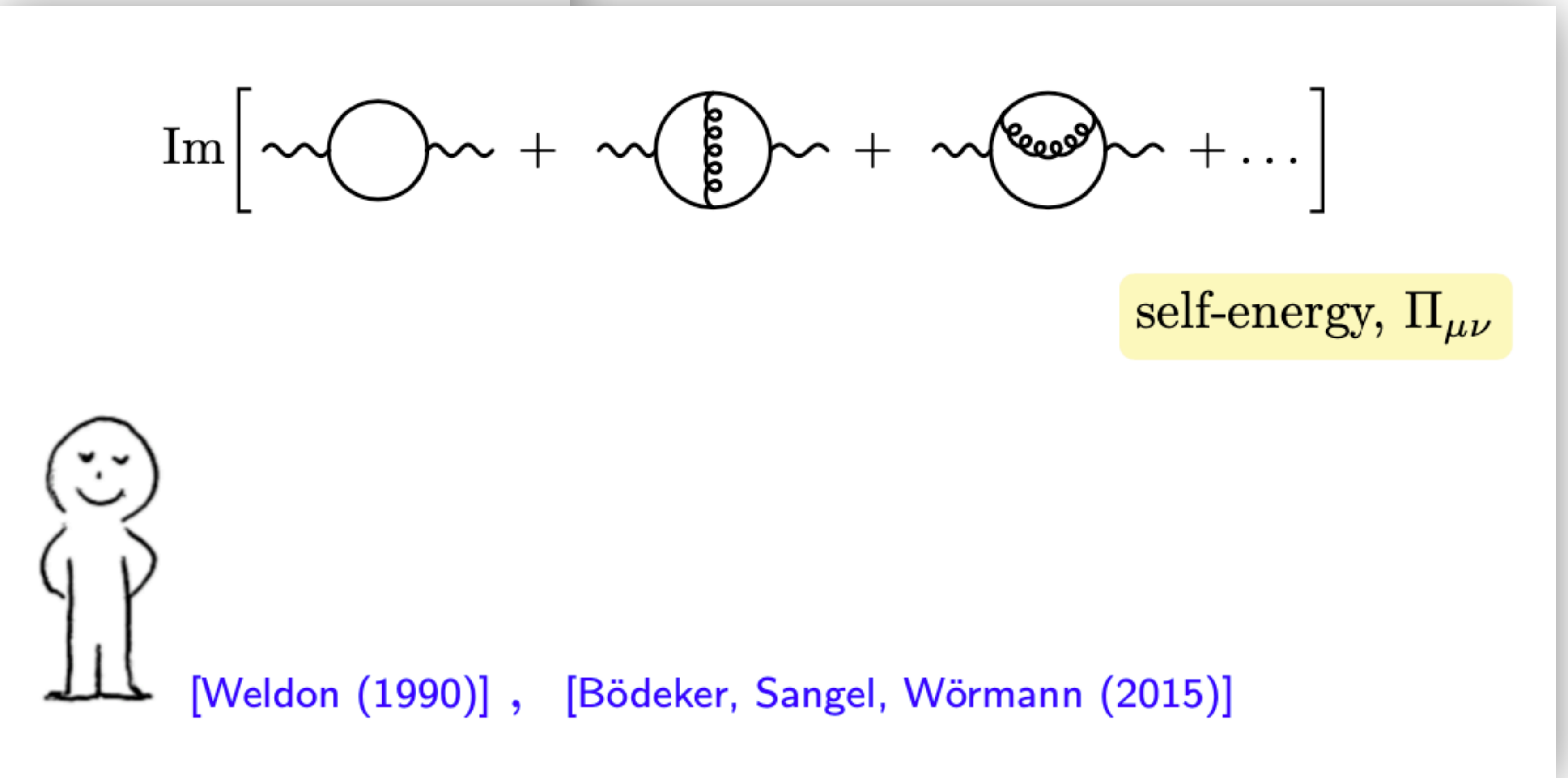

THERMAL DILEPTON AS THERMOMETER

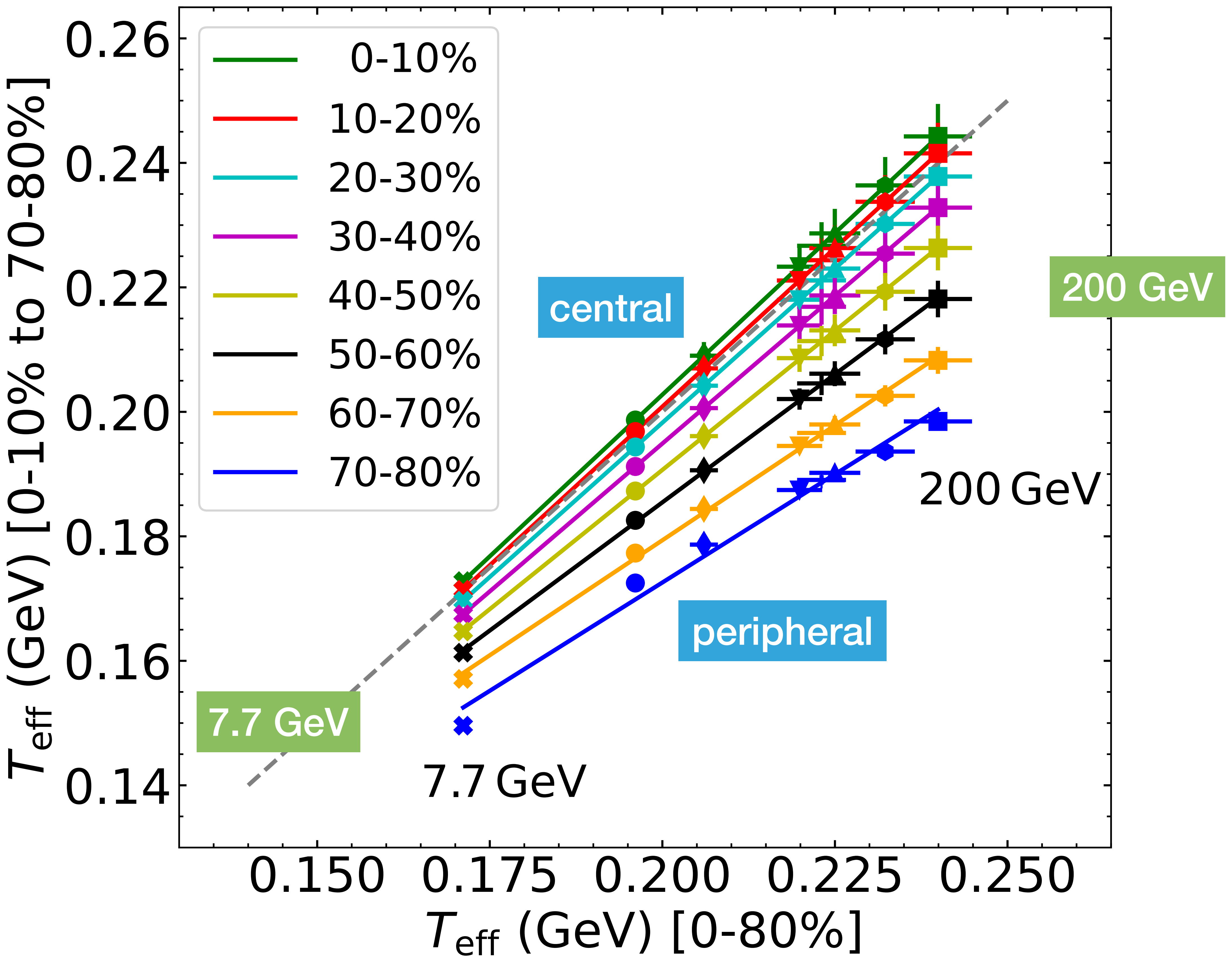

- The effective temperatures extracted from the dilepton spectra in 0-80% centrality are quite close to those in 10-20% centrality across all beam energies